

REFERENCE

NBS
PUBLICATIONS

A11102 247624

NATL INST OF STANDARDS & TECH R.I.C.



A11102247624

Crawford, Myron L./Electromagnetic radlat
QC100 .U56 NO.86-3051 1986 V19 C.1 NBS-P

NBSIR 86-3051

ELECTROMAGNETIC RADIATION TEST FACILITIES EVALUATION OF REVERBERATION CHAMBERS LOCATED AT NSWC, DAHLGREN, VIRGINIA

Myron L. Crawford
Galen H. Koepke

National Bureau of Standards
U.S. Department of Commerce
Boulder, Colorado 80303

June 1986

QC

100

.U56

86-3051

1986

NBSIR 86-3051

ELECTROMAGNETIC RADIATION TEST FACILITIES EVALUATION OF REVERBERATION CHAMBERS LOCATED AT NSWC, DAHLGREN, VIRGINIA

Myron L. Crawford
Galen H. Koepke

Electromagnetic Fields Division
Center for Electronics and Electrical Engineering
National Engineering Laboratory
National Bureau of Standards
Boulder, Colorado 80303

June 1986

Sponsored by
Naval Surface Weapons Center
Dahlgren Laboratories
Dahlgren, Virginia 22448



U.S. DEPARTMENT OF COMMERCE, Malcolm Baldrige, Secretary

NATIONAL BUREAU OF STANDARDS, Ernest Ambler, Director

CONTENTS

	<u>Page</u>
List of Figures and Tables.....	v
1.0 Introduction.....	1
2.0 Description of the NSWC Reverberation Chamber Facilities and NBS Evaluation System.....	2
3.0 Reverberation Chambers Evaluation Results.....	4
3.1 Antenna Coupling Efficiency and VSWR.....	4
3.2 Tuner Effectiveness.....	5
3.3 Test Zone E-Field Uniformity.....	5
3.4 E-Field Amplitude Calibration.....	6
4.0 Comparison of NSWC Reverberation Chambers and NBS Reverberation Chamber.....	7
5.0 Summary of Measurement Uncertainty.....	8
5.1 Estimate of Uncertainty in Establishing E-Field Amplitude Inside the Chambers.....	8
5.2 General Comments.....	10
6.0 Summary and Conclusions.....	11
7.0 Acknowledgments.....	12
8.0 References.....	13

LIST OF FIGURES AND TABLES

- Figure 1. Cross sectional views of NSWC reverberation chamber(s) showing placement of tuner(s), transmitting and receiving antennas, and probe used to evaluate E-field amplitude inside the chamber(s).
- Figure 2. Photographs of interior of NSWC "half" reverberation chamber showing transmitting antennas mounted on side wall and tuner mounted from ceiling.
- Figure 3. Photograph showing closeup of NSWC reverberation chamber tuner.
- Figure 4. Photograph of video monitoring camera mounted inside NSWC reverberation chambers.
- Figure 5. Block diagram of NBS system used in evaluation of NSWC reverberation chambers.
- Figure 6. Statistical representation of the composite VSWR of the transmitting antennas used to launch the fields inside the NSWC reverberation chambers. (see table 1)
- Figure 7. Coupling efficiency (maximum, average and minimum losses) between transmitted and received powers measured at antennas' terminals inside NSWC reverberation chambers. (see table 1 for definition of antennas used.)
- Figure 8. Ratio of maximum to minimum received power obtained by rotating tuner(s) in the frequency range 100 MHz to 18 GHz inside the NSWC reverberation chambers.
- Figure 9. Cross sectional views and photograph of NSWC reverberation chambers showing placement of NBS isotropic probes for evaluation of spatial distribution of E-fields.
- Figure 10. Spatial distribution of the E-field measured inside the NSWC half reverberation chamber using array of 10 NBS isotropic probes: (a) average, and (b) maximum. Net input power normalized to 1 watt. Transmitting antennas are log periodic, 0.1 GHz to 1.0 GHz, and low power horn, 1.0 GHz to 2.0 GHz.
- Figure 11. Spatial distribution of the E-field measured inside NSWC full reverberation chamber using array of 10 NBS isotropic probes: (a) average, and (b) maximum. Net input power normalized to 1 watt. Transmitting antennas same as figure 10.
- Figure 12. Spatial distribution of the E-field measured inside NSWC full reverberation chamber using array of 10 NBS isotropic probes, 100 MHz to 300 MHz: (a) average, and (b) maximum. Net input power normalized to 1 watt. Log periodic transmitting antenna replaced by Cavitenna.

- Figure 13. Average values of the E-field strength measured inside NSWC reverberation chambers using array of 10 NBS isotropic probes with 1 watt net input power: (a) and (c) average of the averages, (b) and (d) average of the maximums. Transmitting antennas same as figure 10.
- Figure 14. Average values of the E-field strength measured inside NSWC full reverberation chamber using array of 10 NBS isotropic probes, 100 MHz to 300 MHz: (a) average of the averages, (b) average of the maximums. Net input power normalized to 1 watt. Log periodic transmitting antenna replaced with cavitenna.
- Figure 15. Average and maximum E-field strength determined inside NSWC reverberation chambers using: (1) composite of three receiving antennas (see table 1) received power measurements, and (2) calibrated 1 cm dipole probe measurements. Net input power normalized to 1 watt.
- Figure 16. Average and maximum E-field strength inside empty NBS reverberation chamber for 1 watt net input power determined from: (1) composite of 3 antennas received power measurements, and (2) calibrated 1 cm dipole probe measurements.
- Figure 17. Comparison of the peak responses of NBS 1 cm dipole probe and NBS single ridged horn to normalized E-field of 37 dB V/m determined using NBS and NSWC reverberation chambers. (a) 1 cm dipole probe, (b) ridged horn.
- Table 1. Transmitting and receiving antennas used in the NSWC reverberation chambers evaluation.
- Table 2. Spatial variations in the E-field average and maximum values measured inside the NSWC reverberation chambers.
- Table 3. Summary and estimates of measurement uncertainties for determining field strength inside NSWC reverberation chambers - Mode Tuned (100 MHz - 2.0 GHz).
- Table 4. Summary and estimates of measurement uncertainties for determining field strength inside NSWC reverberation chambers - Mode Stirred (1.0 GHz - 18.0 GHz).
- Table 5. Estimates of impedance mismatch uncertainties for received power measurements for NSWC reverberation chambers.

Electromagnetic Radiation Test Facilities
Evaluation of Reverberation Chambers
Located at NSWC, Dahlgren, Virginia

Myron L. Crawford
Galen H. Koepke

Electromagnetic Fields Division
National Bureau of Standards
Boulder, Colorado 80303

This report describes measurement procedures and results obtained from evaluating the reverberation chamber facilities located at the Naval Surface Weapons Center (NSWC), Dahlgren, Virginia. The two chambers tested are referred to as 1) the half chamber, and 2) the full chamber. The facilities were developed by the NSWC for use in measuring and analyzing the electromagnetic susceptibility/vulnerability (EMS/V) of weapon systems and the shielding effectiveness of enclosures and shielding materials. A brief description of each facility is given including the instrumentation used for performing the evaluation and calibration of the facilities by the National Bureau of Standards (NBS). Measurements described include: 1) evaluation of the chambers' transmitting and receiving antennas' voltage standing wave ratios; 2) measurement of the chambers' insertion loss or coupling efficiency versus frequency; 3) measurement of the chambers' tuner effectiveness; 4) determination of the E-field uniformity in the chambers' test zones versus frequency; 5) determination of the absolute amplitude calibration of the test E-fields in the chambers based upon the reference antennas received power measurements and calibrated dipole probe antenna measurements; and 6) comparison of reference equipment under test (EUT) responses to test fields established inside the NSWC reverberation chambers and the NBS reverberation chamber. These results can then be compared to anechoic chamber results. Conclusions given indicate that the NSWC chambers can be used at frequencies down to approximately 150 MHz. Estimates are given of the measurement uncertainties derived empirically from the test results.

Key words: electromagnetic radiated susceptibility/vulnerability measurements; reverberation chamber.

1.0 Introduction

The use of a reverberation chamber for performing EMS/V measurements is relatively new. Considerable work has been done in the past to evaluate and document methods for using this technique [1-4]. Recently, considerable research work has been done at the National Bureau of Standards (NBS) to

carefully evaluate, develop (when necessary), describe, and document the methodology for performing radiated susceptibility/vulnerability (EMS/V) measurements using a reverberation chamber. This effort is described in an NBS publication, NBS TN 1092 [5]. The incentive for performing this work stems from the numerous advantages suggested for the use of a reverberation chamber. These include:

1. Electrical isolation from or to the external environment;
2. Accessibility (indoor test facility);
3. The ability to generate high level fields efficiently over large test volumes;
4. Broad frequency coverage;
5. Cost effectiveness;
6. Potential use for both radiated susceptibility and emission testing with minor instrumentation changes;
7. No requirement of physical rotations of the equipment under test (EUT);
8. Security; and
9. Personnel not exposed to radiated test fields.

These advantages are somewhat offset by limitations which include loss of polarization and directivity information relative to the EMC/EMI profile of the EUT and somewhat limited measurement accuracy. However, this technique does offer a time-efficient, cost-effective way to evaluate the EMS/V performance of large equipment using a shielded enclosure with minor modifications. The measurement concept utilizes the shielded, high-Q, multimoded environment to obtain uniform (time averaged) fields that may simulate "real world", near field environments. Also, it may well be the only technique by which very high exposure fields can be safely generated for performing EM susceptibility tests required by the Department of Defense for some of their "real world" applications.

These considerations, along with others, motivated the Naval Surface Weapons Center, Dahlgren, VA to invest in the research and development of this methodology and finally to construct and place into operation the facilities whose description and evaluation are given in this report. Measurements described were performed between May 10 and May 31, 1985.

2.0 Description of the NSWC Reverberation Chamber Facilities and NBS Evaluation System

The NSWC reverberation chambers are made from one large shielded enclosure partitioned into two compartments with a double walled bulkhead removable panel. The two chambers evaluated consist of: 1) the "half chamber", 3.51 m x 5.18 m x 5.86 m in size (which is actually a little over half of the full size enclosure), and 2) the full chamber, 3.51 m x 5.18 m x 10.82 m in size. The enclosure is constructed of continuous welded steel sheeting similar to the NBS reverberation chamber [5]. It is equipped with two large 2.13 m x 2.13 m air inflatable sliding doors located at each end for access into the two compartments when the partition is in place. Each compartment has its own tuner as shown in figure 1. Typically only the larger of the two compartments (half chamber), or the full size chamber are used for performing EMS/V tests. The particular chamber in use (half or full) is excited by transmitting antennas located either close to a corner,

oriented toward the corner (150 MHz - 1.0 GHz), or on the side wall of the chambers oriented toward the tuner (1.0 GHz - 18 GHz) as shown in figures 1 and 2. Forty-five degree waveguide elbows are used at frequencies above 8.0 GHz. The purpose of these antenna placements is to couple the transmitted signal into all possible chamber modes as efficiently and uniformly as possible without favoring particular modes or transmitting directly into the chamber's test zone, or coupling the signal directly between the transmitting and receiving antennas. This is necessary to obtain a uniform, statistical, spatial distribution of the field in the chamber's test zone. A single tuner, mounted from the ceiling (figures 2 and 3) was used for the half chamber evaluation tests. A second tuner, also ceiling mounted, was activated for the full chamber evaluation tests. The chambers have remote video monitoring equipment shown in the photograph of figure 4. This equipment is EMI hardened and was left in the chambers during the evaluation tests. The reference receiving antennas (used for determining the field strength in the chamber) are placed in and oriented toward one corner of the chamber as shown in figure 1. The transmitting and reference receiving antennas used within their specified frequency bands are identified in Table 1.

The chambers were evaluated using two different operational approaches referred to as mode-tuned and mode-stirred [5]. The mode-tuned approach was used at frequencies from 100 MHz to 2 GHz, and the mode-stirred approach was used at frequencies from 1.0 GHz to 18 GHz.

For the mode-tuned tests, the tuner is stepped at selected, uniform increments, permitting measurements of the net input power supplied to the transmitting antenna, the receiving antenna power, field-measuring probes responses and the EUT response at each tuner position. This allows corrections to be made for the changes in the transmitting antenna's input impedance as a function of tuner position and frequency so that the measurement results can be normalized to a constant net input value (1 watt for these tests). The number of tuner steps per revolution used were 200 at frequencies below 1.0 GHz and 400 in the frequency range 1 - 2 GHz.

For the mode-stirred tests, the tuner is continuously rotated while sampling the reference antenna received power, field probe response and the EUT response at rates much faster than the tuner revolution rate. These measurements are made using a spectrum analyzer, diode detectors, and "smart" voltmeters that are capable of data storage and calculation of statistical functions such as mean values and standard deviations. The mode stirred approach allows large data samples (up to 9,999) to be obtained for a single tuner revolution. Tuner revolution rates can be adjusted to meet the EUT output monitor and diode probe response time requirements. Typical rates used are approximately 3 to 6 minutes per revolution.

A block diagram of the basic system used to evaluate the chambers is shown in figure 5. The test field was established inside the chamber under evaluation by means of an rf source connected to the appropriate transmitting antenna defined in table 1. Modes excited inside the chamber were then stirred by rotating the tuner(s) which function as field-perturbing devices. The test zones in the chambers were defined as the chambers' volume less a minimum separation from the walls, and ceiling of 1/2 meter. Placement of an EUT should fall within this volume except possibly relative to the floor which may be less than 1/2 meter depending

upon the EUT intended use configuration relative to ground planes. Test leads and cables were routed to appropriate monitors, etc., outside the chambers via shielded feed-through connectors, and high resistance lines. This was done to prevent leakage of fields to the outside environment. A precision 10 dB attenuator was used whenever possible, between the power detector or spectrum analyzer and the receiving antenna. This was done to minimize impedance mismatch with the receiving antenna. A calibrated bidirectional coupler was used at the input to the transmitting antenna to allow measurements of the net input power. For mode stirred measurements, the net input power was measured only at the beginning of the measurement cycle. Details of how the measurement cycles proceed under computer control, and how the data are recorded, managed, and processed for presentation are contained in [5].

3.0 Reverberation Chambers Evaluation Results

How well a shielded enclosure can be made to operate as a reverberation chamber depends upon a number of interacting considerations. The major requirement is that the enclosure be large compared to the wavelength of the lowest frequency intended for use so that sufficient modes, necessary to obtain statistical spatial field uniformity, exist. This should be true for the NSWC chambers described above at frequencies above approximately 100 MHz.

3.1 Antenna Coupling Efficiency and VSWR

The efficiency with which energy can be injected into or coupled out of the chamber via the transmitting and receiving antennas is determined by: 1) the voltage standing wave ratio (VSWR) of the antennas (i.e., the impedance match between the rf source and the transmitting antenna or between the receiving antenna and its output detector), and 2) the ability of the antennas to couple energy into or out of the particular modes that exist at the test frequencies of interest. Rotating the tuner changes the chamber's boundary conditions and hence, shifts the mode excitation frequencies. This, of course, changes the characteristics of the field inside the enclosure which in turn influences the effective VSWR of the antennas. For example, if the tuner is rotated, the VSWR of the transmitting antenna is affected and hence the net input power to the enclosure is changed. This can result in errors in determining the amplitude of the field inside the enclosure. Variations (determined by a statistical approach) in the VSWR of the transmitting antennas used to excite the NSWC half and full size chambers are shown in figures 6a and 6b. The receiving antennas VSWRs should be similar. The figures show the maximum, average, and minimum VSWR obtained by rotating the tuner through a complete cycle at discrete frequencies from 100 MHz to 18 GHz. Large variations exist, especially at frequencies below 1 GHz. At higher frequencies the variations become comparatively negligible approaching the open field VSWR of the antennas.

The coupling efficiency of the antennas placed inside the chambers is expressed in terms of a ratio of the net input power delivered to the transmitting antenna to the power available at the terminals of the receiving antenna. These ratios, referred to as chamber loss, are shown in figures 7a and 7b for the half and full size chambers. The curves shown in

each figure are the maximum, average, and minimum losses as a function of frequency, determined by rotating the tuner through a complete revolution. Impedance mismatch between the power detector used to measure the received power and the receiving antenna have not been accounted for. As noted from the data shown in figures 6, this can contribute to a significant error, especially at frequencies below 1 GHz. The magnitude of this source of error is discussed in [5] and is included in the error estimates given in section 5 of this report.

3.2 Tuner Effectiveness

Another consideration in the operation of a reverberation chamber is the effectiveness of the tuner to redistribute the energy in the chamber and hence to obtain complete randomness in the characteristics of the test signal. To achieve this the tuner must be electrically large and be shaped or oriented so as to distribute energy equally well into all possible chamber modes. A test to determine how well the tuner is functioning is to measure the ratio of the maximum to minimum received power of the receiving antenna as a function of tuner position. This is done while maintaining a constant net input power to the chamber's transmitting antenna. A large ratio indicates the tuner is, in fact, redistributing the scattered fields inside the chamber effectively. The results of these measurements are given in figures 8a and 8b for the half and full chambers. A number of factors, including those referred to earlier related to the design of the tuner, can influence the magnitude of this ratio. For example, a reduction in this ratio after placing the EUT inside the chamber is an indication of the loading effect or reduction of the chamber's quality factor (Q) caused by the EUT. A minimum ratio of 20 dB is suggested for proper operation of the chamber.

3.3 Test Zone E-Field Uniformity

Tests were made to determine the E-field uniformity in the chambers as a function of spatial position and frequency. Ten NBS isotropic probes designed to operate at frequencies up to 2 GHz were placed inside each chamber as shown in figures 9a, 9b, and 9c. Each probe has three orthogonally oriented dipoles aligned with the enclosures' axes. Measurements were made of the field strength of each orthogonal component at the ten locations for each tuner position (200 steps of 1.8 degrees for frequencies 100 - 1000 MHz, and 400 steps of 0.9 degrees for frequencies 1.0 - 2.0 GHz). These data were normalized for a net input power of 1 watt applied at the input terminals of the transmitting antennas. The maximum and average values for each component and the vector sum (total) of the components were then determined from the complete data sets. The results of these measurements are shown in figures 10 and 11. The spread of the data shows the spatial field variation inside the enclosure at the indicated frequencies. A substantial drop in the field strength is indicated at 100 MHz. Additional measurements were made using a different transmitting antenna to determine if this drop was due to the low frequency, (out-of-band) response characteristics of the transmitting antenna used or due to insufficient moding of the chambers at 100 MHz. These additional measurements were made only in the full chamber since its larger volume should allow greater moding and hence lower frequency use. The antenna selected to replace the transmitting antenna used to obtain the data of figures 10 and 11 was designed to operate in the frequency range 30 to 1000

MHz. The antenna's lower frequency limit is well below the 100 MHz anticipated lower frequency limit for the full size chamber. Results of the measurements are shown in figure 12. A comparison of these results with figure 11 indicate the chamber is operating properly down to 100 MHz. The drop in E-field indicated in figure 11 at 100 MHz is believed then, to be due to the out of band response characteristics (poor VSWR and/or efficiency) of the log periodic antenna used in obtaining the data of figures 10 and 11. The spread in the data (spatial distribution) at selected frequencies is summarized in table 2. The spread is as great as ± 8 dB at 100 MHz (half chamber) decreasing to approximately ± 3.5 dB at 300 MHz, ± 2 dB at 1.0 GHz, and ± 1.5 dB at 2.0 GHz. The average values, determined statistically from the data measured at the ten locations, for the average and maximum E-fields of each component and their composite total are summarized in figures 13 and 14. Note that the relative amplitudes of the field components are approximately the same and the composite total of the average E-field components is approximately 4.8 dB or a ratio of $\sqrt{3}$ greater than the individual components. This indicates the measured values of the average of each component are independent of polarization in the chamber. Hence, the average field inside the chambers appears to be randomly polarized. The composite total however, of the E-field components' maxima (figures 13b, 13d, and, 14b) are less than 4.8 dB. This indicates that the maximum measured values for each component are not independent (i.e., $E_x(\text{total})$ is a function of $E_y(\text{total})$, etc.). This is similar to the results obtained in the NBS reverberation chamber and appears to be inherent in the reverberation chamber measurement method. The implication is that if multiple receptors are involved in establishing the maximum susceptibility of an EUT (for example in measuring the E-field in the chamber by using an isotropic probe with 3 orthogonal dipoles), the difference between the maximum and average response determined for the EUT may be incorrectly weighted (less than the 7-8 dB anticipated). (See section 2.3 of [5].)

3.4 E-Field Amplitude Calibration

The field strength in the chamber can be determined in two ways. The first is to measure the power received by the reference antennas, and then determine the equivalent power density in the enclosure using the equation [5],

$$\bar{E}_a = \sqrt{\bar{\eta}' \bar{P}_d'} \approx \frac{4\pi}{\lambda} \sqrt{30 \bar{P}_r'} \quad (\text{V/m}), \quad (1)$$

where \bar{E}_a is the equivalent electric field, $\bar{\eta}'$ is the statistically averaged wave impedance in the chamber, \bar{P}_d' is the equivalent power density in the enclosure, λ is the wavelength, and \bar{P}_r' is the average measured received power. The averaged wave impedance is assumed to be approximately equal to 120π ohms. The validity of (1) has been verified and is discussed in section 2.3.1 of NBS TN 1092 [5].

The maximum and average electric field strengths inside the NSWC chambers determined from the receiving antenna power measurements and (1)

are shown in figures 15a and 15b. These data were obtained for a 1 watt net input power to the enclosure's transmitting antenna.

The electric field strength inside the chambers can be determined a second way by measuring it with one or more calibrated probes. Data obtained using a 1 cm dipole probe fabricated at the NBS are also shown on figures 15a and 15b. The probe was calibrated in a planar field using a TEM cell [6] at frequencies up to 500 MHz and in an anechoic chamber at frequencies from 500 MHz to 18 GHz [7]. The assumption is made that the field strength over the aperture of the probe inside the reverberation chambers will approximate the planar field used to calibrate the probe. This is reasonable, at least at frequencies for which the probe is electrically small. Also, the open-space far-field gain of an electrically small dipole is small (1.76 dB). Thus, the probe-measured fields should be equivalent, within approximately 1.76 dB, to the E-fields determined using a receiving antenna. This is true if the equivalent gains for the probe and receiving antenna, after being placed inside the chambers, are assumed to be unity. The agreement shown is typical of the random variations in the data used to determine the field strength inside the reverberation chambers.

4.0 Comparison of NSWC Reverberation Chambers with NBS Reverberation Chamber

Since the NSWC chambers are very similar to the NBS chamber (all are constructed of continuous welded steel sheeting), it is of value to compare evaluation results obtained for the different chambers. Such a comparison was made to answer two significant questions. First, can the input power requirements of a chamber as a function of its size be estimated based upon the calibration of a chamber of similar construction, and second, are susceptibility test results obtained for the same EUT in different reverberation chambers comparable? Results shown in figures 16 and 17 indicate that both questions are answered in the affirmative. Figure 16 shows the fields inside the NBS chamber calculated from the chambers' reference antenna received power measurements and also measured by the calibrated 1 cm long dipole probe. These data can then be compared with figures 15a and 15b showing the same type data for the NSWC chambers. The net input power was normalized to one watt for all three chambers. The field inside the NBS chamber is approximately 4 dB stronger than the NSWC half chamber and 6 dB stronger than the NSWC full chamber. It is interesting to recall from theory that the power density inside a second chamber can be estimated from a calibrated chamber by using the equation [5],

$$\frac{P_{d_1}}{P_{d_2}} = \frac{V_2 Q_1}{V_1 Q_2} , \quad (2)$$

where P_d is the power density, V is the volume and Q is the quality factor for the particular chamber (1 or 2). If we assume the first chamber is the NBS chamber with a volume, $V_1 = 38.19$ cubic meters and $Q_1 = 0.548/\delta_1$, and the second chamber is the larger, full size NSWC chamber with a $V_2 = 196.73$

cubic meters and $Q_2 = 0.887/\delta_2$, the ratio in average power densities (assuming the same net input power and the same metal, $\delta_1 = \delta_2$), $P_{d_1}/P_{d_2} =$

3.22. (The parameter, δ , is the skin depth of the metal used in the enclosures.) The average power density inside the larger chamber would be approximately 1/3.22 or 0.311 times as much as that in the NBS enclosure. This is equal to about 5 dB, a little less than the approximate 6 dB difference indicated by comparing figures 15b and 16, but still within reason.

The positive answer to the second question, that of obtaining comparable susceptibility results using different chambers, is demonstrated in figures 17a and 17b. These graphs show the comparison in measuring the responses of the NBS 1 cm dipole probe and a rectangular single ridged horn to a normalized 37 dB V/m field inside the 3 different reverberation chambers. Comparisons of the estimated curve fits for each data set agree quite well (within approximately 2 dB).

An effort was also made to compare results obtained, for the two reference standard EUT referred to above (section 4), between the reverberation chambers and an anechoic chamber to estimate a "correlation factor." The results consisted of the measured peak output response of two EUTs exposed to test fields in the two environments of the same relative amplitude. The anechoic chamber used was a 4.9 m x 6.7 m x 8.5 m chamber lined with 66 cm high-frequency rf absorber located at NBS, Boulder, Colorado. The EUTs were designated as references because they are simple structures that can be accurately characterized both theoretically and experimentally. The outcome of this effort can be found in NBS TN 1092 [5].

5.0 Summary of Measurement Uncertainty

5.1 Estimate of Uncertainty in Establishing E-Field Amplitude Inside the Chambers

Susceptibility/vulnerability test fields established inside the chamber(s) can be determined two ways: either using a reference receiving antenna or a calibrated probe. If a reference receiving antenna is used, the field is determined in terms of "equivalent" power density or "equivalent" electric field strength by using (1). If a calibrated E-field probe is used, the field strength is measured relative to an equivalent probe response in a known planar field. An estimate of the uncertainties in each of these methods can be determined by analyzing the contributing parameters involved in each method. The significant sources of error are summarized in tables 3 and 4 for the mode-tuned and mode stirred approaches respectively, within their appropriate frequency bands. Four major categories are identified. The first is the uncertainty in determining the received power measured by the reference antennas, (1a. tables 3 and 4), or in measuring the E-field with the calibrated probe, (1b. tables 3 and 4). The uncertainty in determining the received power is broken up into five components: cable loss, attenuator calibration, reference antenna efficiency, power meter or spectrum analyzer measurement uncertainties, and impedance mismatch. Values shown for the first four components are typical of estimated uncertainties stated for these types of measurements and instruments. The fifth component, impedance mismatch is the uncertainty in

determining the actual power delivered to the detector (load) attached to the antenna (source) relative to the power available. The actual or measured power is a function of the impedance match between the source and load, with maximum power transfer occurring when a conjugate impedance match exists.

Power transfer between a source and a load is given as

$$P_f = \frac{\text{fraction of maximum available power absorbed by the load}}{\text{by the load}} = \frac{(1 - |\Gamma_S|^2)(1 - |\Gamma_L|^2)}{|1 - \Gamma_S \Gamma_L|^2}, \quad (3)$$

where Γ_S and Γ_L denote complex reflection coefficients for the source and load respectively. The magnitudes, $|\Gamma_S|$ and $|\Gamma_L|$ can be obtained from the appropriate VSWR by the expressions

$$|\Gamma_i| = \frac{\text{VSWR} - 1}{\text{VSWR} + 1}, \quad i = S \text{ or } L.$$

The VSWRs for the reference antennas (sources) and power detectors (loads) used in the NSWC reverberation chambers are given in table 5. These values were used to calculate the estimated uncertainties shown for the mismatch errors in tables 3 and 4. Both the statistical average and maximum values are given.

Discussions of the uncertainty in calibrating E-field probes in planar fields can be found in [6,7]. Their response to fields inside a reverberation chamber has been shown to be less than their response in a planar field. The difference is proportional to their free-space gain [4]. Typical probes used are electrically short dipoles over most of the frequency range. Sometimes however, they are used beyond their resonance frequency (for example the 1 cm dipole probe at frequencies above 15 GHz). The corrections needed to correlate results obtained in the reverberation chambers with those obtained in free-space or in anechoic chambers then correspond to from 1.76 dB to 2.6 dB. The total estimated uncertainties of using the NBS 1 cm dipole probe to measure E-field amplitudes in the reverberation chambers are shown on tables 3 and 4 (see 1b).

The second category of error, referred to as mixing or sampling efficiency, is divided into two parts. The first part relates to the ability to obtain a uniform spatial field distribution (statistically) inside the chamber and to effectively destroy the polarization characteristics of the exposure field. (i.e., the statistically determined response characteristics of the EUT and chamber reference antenna are independent of their directional properties.) The second part is the uncertainty due to limiting the number of tuner positions per revolution when performing the measurement. This source of uncertainty is different when determining the average as compared to the maximum field as shown in the tables. Data contained in [5] (figure 2.27 and table 6.4) were used in obtaining these estimates.

The third category of uncertainty relates only to determining the equivalent E-field strength in the chamber from the equivalent power density. Recall that equation (1) assumes that the equivalent wave impedance inside the chamber is 120π ohms. In reality this is not true as has been shown [5]. However, data shown in [5] can be and were used to provide an estimate for this error. These data indicate that a wave impedance as great as 1600 ohms can exist at frequencies below 500 MHz when the maximum E-field is measured. This corresponds to approximately 6 dB of correction. However, a significant amount of data obtained to date, indicates that a well behaved relationship (7-8 dB difference) exists between the measured peak and average values of the E-field. This suggests, at least at frequencies above a few hundred megahertz where the chambers are highly moded, that the peak value of the wave impedance for the maximum measured E-field inside the chambers decreases as the frequency increases. In the limit, it is believed the value approaches 120π ohms. Thus this source of error decreases as frequency increases. These observations are reflected in the uncertainty estimates shown in the tables.

The fourth source of error occurs if one fails to correct for net input power variations due to the loading effect of the chamber on the VSWR of the source antennas. These corrections are made when using the mode-tuned approach and hence are not included in table 3. They are not made however, when using the mode-stirred approach and hence are shown in table 4.

The total worst-case uncertainties for each method (receiving antenna and calibrated probe) of determining the E-field for both the mode-tuned and mode-stirred approaches are shown at the bottom of the appropriate table. These uncertainties should be regarded as a conservative estimate. The probability of the true value of amplitude of the test field being near an extreme is small. This is because the probability of all error sources being at their extreme value in the worst possible combination is almost zero.

A more realistic method of combining uncertainties is the root-sum-of-the-squares (RSS) method. The RSS uncertainty is based on the fact that most of the errors are statistically independent of each other and hence combine like random variables.

Finding the RSS uncertainty requires that each individual uncertainty be expressed in fractional form. The method of calculation follows the name - square the components, sum those squares and then take the square root. The results for both methods of determining the E-fields are shown at the bottom of tables 3 and 4.

5.2 General Comments

Some general comments on interpreting uncertainties of immunity measurement results based upon the above experimental error analysis are appropriate.

- 1) The mismatch error at frequencies below 2 GHz, (particularly if corrections are not made for the transmitting or receiving antennas mismatches looking into their source or load), will cause the field determination inside the chamber to be low. This also causes the EUT

response results to be lower than they actually are. For example, the low frequency data of figures 17a and 17b should be corrected (response increased) proportionally to the systematic offset error estimates shown in tables 3 and 4.

- 2) The wave impedance, when the peak response of an EUT is measured, appears to be higher than 120π ohms. This means that if the free space wave impedance of 120π ohms is used in determining the corresponding peak amplitude of the exposure field, there will be a systematic offset error resulting in too low a calculated E-field exposure value. Since the actual E-field is higher than the calculated value this results in too high a EUT response indication for a specified E-field exposure. If the E-field is determined using a calibrated E-field probe, there still remains a degree of uncertainty since the wave impedance is different in the calibration environment as compared to the reverberation chamber environment. For this reason, this source of error was included in calculating the total and RSS uncertainties in establishing the E-field using the probe method.
- 3) The spatial variation in the measured, statistically determined E-field in the chambers resulting from a complete revolution of the tuner(s) decreases from as great as ± 8 dB at 100 MHz to less than ± 2 dB at 2.0 GHz. It is expected that this variation will continue to decrease as the frequency increases. However, high variations exist in the response data obtained for the reference standard EUT (1 cm dipole and ridged horn) at frequencies where the spatial E-field variation are small. This is due to the other contributing sources of error as discussed in 5.1. A way to reduce this problem is to increase the number of frequencies at which data are taken (clustered around a particular frequency of interest) or increase the number of reference receiving antennas or probes used to determine the exposure field and then average the data (for example as was done in figures 13 and 14).

6.0 Summary and Conclusions

1. The practical lower frequency limits recommended for using the NSWG half and full size chambers, assuming the transmitting antennas listed in table 1 are used, are approximately 200 MHz and 150 MHz respectively.

2. Spatial variations in the E-field maximum and average values determined in the half and full chamber test volumes are shown in table 2. These data were determined using the mode-tuned approach with 200 tuner increments at 100 MHz to 1000 MHz and 400 tuner increments at 1000 MHz to 2000 MHz for one complete tuner revolution. The limitation for determining the spatial E-field variation is most likely due to the increasing mode density and hence field complexity in the chamber as a function of frequency. The limited sample size then becomes insufficient to determine the actual maximums with greater accuracy. In reality, the spatial E-field variations should continue to decrease (less than ± 1.8 dB) above 2 GHz if sufficiently large data samples are taken and the measurement instrumentation has adequate dynamic range and precision.

3. Antennas used within the chambers for transmitting energy or for determining the test E-field amplitude should not be used outside their recommended frequency range. See table 1 for antennas recommended for the NSWC chambers.

4. The mode-tuned approach is recommended for use in both chambers at frequencies below 1 GHz. Either mode-tuned or mode-stirred can be used from 1 to 2 GHz. The mode stirred approach is recommended for use above 2.0 GHz. This allows for some overlap in the measurement approach selected. Based upon antenna VSWR and EUT response data obtained from evaluation measurements, the following approaches and number of samples per tuner(s) revolution are suggested for performing susceptibility testing.

Frequency Range	Method	# Tuner Positions/Samples
0.15 - 1.0 GHz	Mode Tuned	200
1.0 -- 2.0 GHz	Mode Tuned	400
1.0 -- 4.0 GHz	Mode Stirred	>3000
4.0 - 18.0 GHz	Mode Stirred	>5000

5. The maximum E-field is approximately 8 dB greater than the average E-field established inside the chambers.

6. The theory for predicting input power requirements for a second unknown chamber based upon the known requirements of a first chamber appears to be valid.

7. EMS/V data obtained for an EUT in similarly constructed, but different reverberation chambers, are approximately the same.

8. Since results of EUT response measurements made using the NSWC reverberation chambers are approximately the same as for the NBS reverberation chamber, it follows that these results will be lower than when measured in the open field or in anechoic chambers. The "correlation factor" appears to be the open space (far-field) gain of the EUT. This implies that susceptibility criteria determined for an EUT using a reverberation chamber must include an additional factor proportional to the EUT's open-field estimated maximum gain as a function of frequency.

9. Also implied from 7 above is that the directional characteristics of an antenna or EUT placed inside a reverberation chamber are lost, resulting in an equivalent gain in this complex environment of unity.

7.0 Acknowledgments

Work described in this report was sponsored by the Naval Surface Weapons Center, Dahlgren, Virginia, with Mr. John Bean as project monitor. The authors wish to acknowledge the assistance of Mr. Bean and Mike Hatfield, NSWC, Lawrence C. Halley, EG&G, Washington Analytical Services Center Inc., Dahlgren, Virginia and John Workman, NBS for their help and cooperation in performing the measurements discussed in this report. In addition, the authors express appreciation to Dr. Mark Ma, NBS for his support, helpful comments and editorial review.

8.0 References

- [1] Mendes, H.A. A new approach to electromagnetic field-strength measurements in shielded enclosures. Wescon Tech. Papers; Los Angeles, CA. 1968 August.
- [2] Cummings, J.R. Translational electromagnetic environment chamber, a new method for measuring radiated susceptibility and emissions. Proc. IEEE Int. Symp. on EMC; 1975; San Antonio, TX.
- [3] Corona, P.; Latmiral, G.; Paolini, E.; Piccioli, L. Performance of a reverberation enclosure for power measurements in the microwave range. 2nd Symp. Tech Exhibition on EMC; 1977; Montreux, Switzerland.
- [4] Bean, J.L.; Hall, R.A. Electromagnetic susceptibility measurements using a mode-stirred chamber. Proc. IEEE Int. Symp. on EMC; 1978; Atlanta, GA.
- [5] Crawford, M.L.; Koepke, G.H. Design, evaluation and use of a reverberation chamber for performing electromagnetic susceptibility/vulnerability measurements. Nat. Bur. Stand. (U.S.) Tech. Note 1092; 1986 April. 148 p.
- [6] Crawford, M.L. Generation of standard EM fields for calibration of power density meters: 20 kHz to 1000 MHz. Nat. Bur. Stand. (U.S.) NBSIR 75-804; 1975 January. 40 p.
- [7] Crawford, M.L.; Koepke, G.H. Comparing EM susceptibility measurement results between reverberation and anechoic chambers. IEEE Inter. Symp. on EMC; 1985; Wakefield, MA.

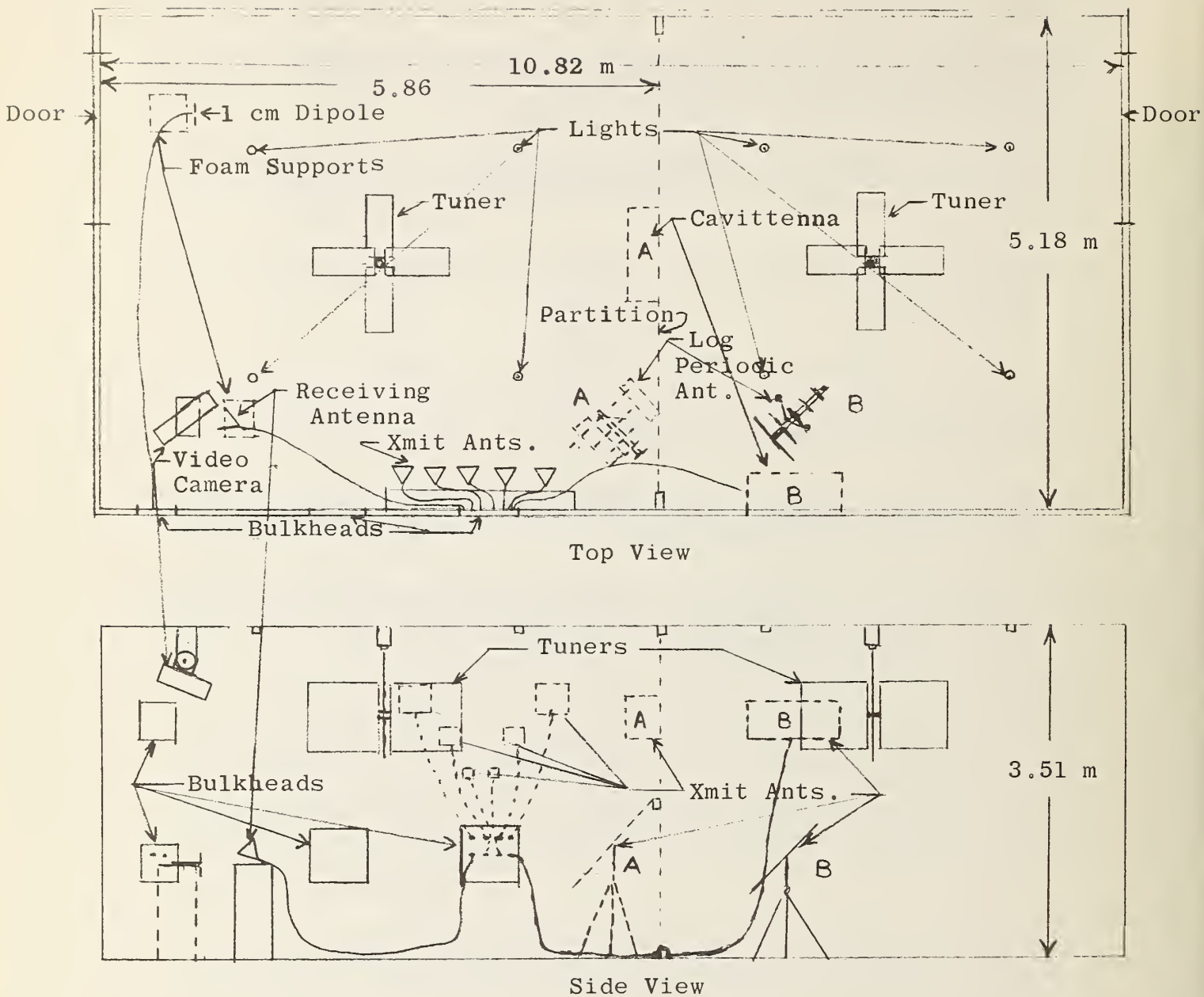


Figure 1. Cross sectional views of NSWC reverberation chamber(s) showing placement of tuner(s), transmitting and receiving antennas, and probe used to evaluate E-field amplitude inside the chamber(s). Cavittenna and log periodic antennas used in location A for half chamber when partition is in place. Cavittenna and log periodic antennas used in location B for full chamber when partition is removed. Antennas on side wall remain in place for either chamber configuration (half or full).

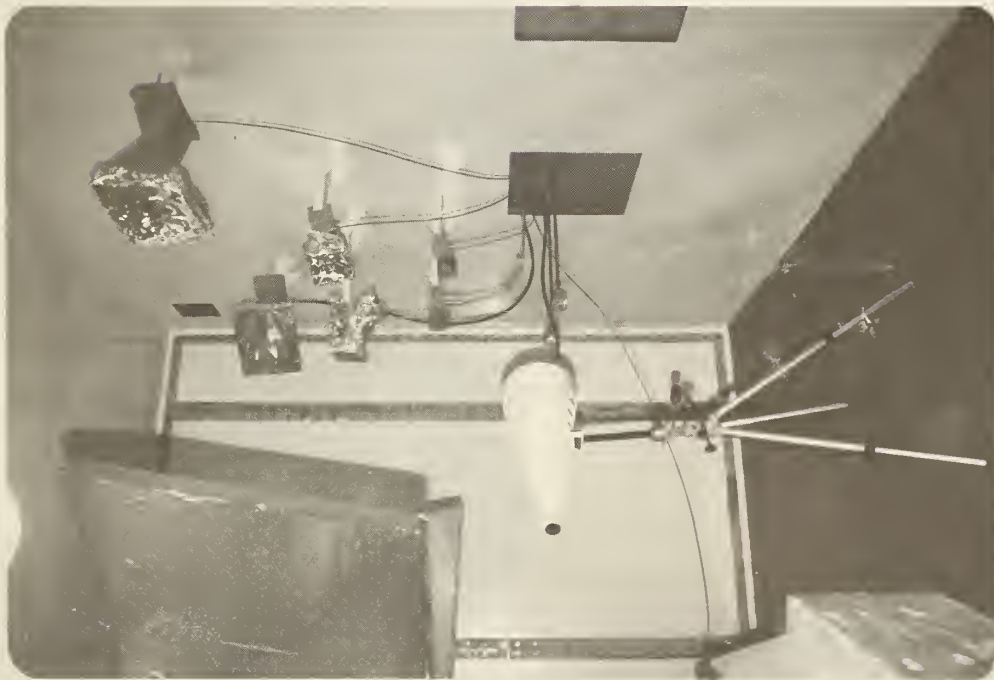


Figure 2. Photographs of interior of NSWC "half" reverberation chamber showing transmitting antennas mounted on side wall and tuner mounted from ceiling.

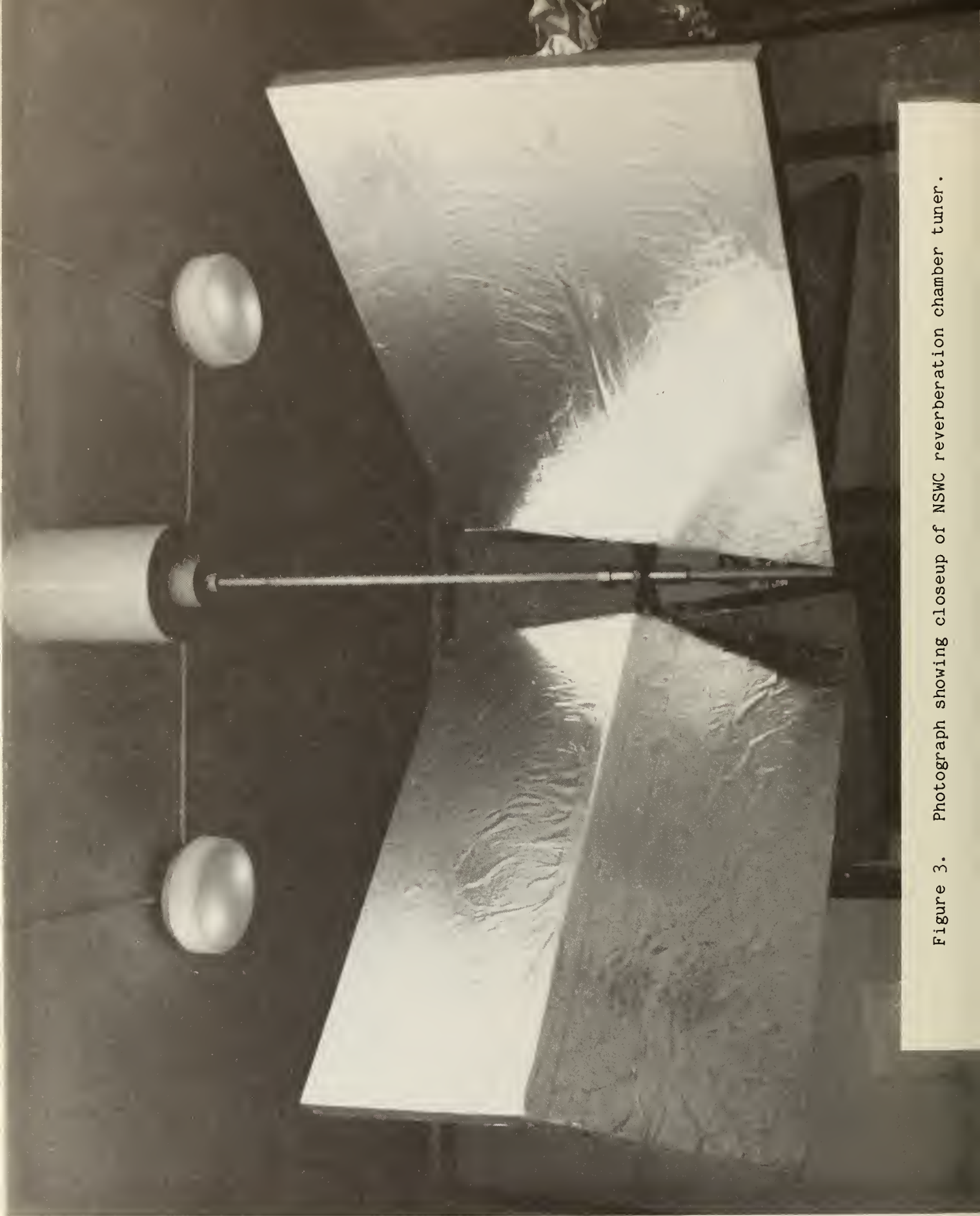


Figure 3. Photograph showing closeup of NSWC reverberation chamber tuner.



Figure 4. Photograph of video monitoring camera mounted inside NSWC reverberation chambers.

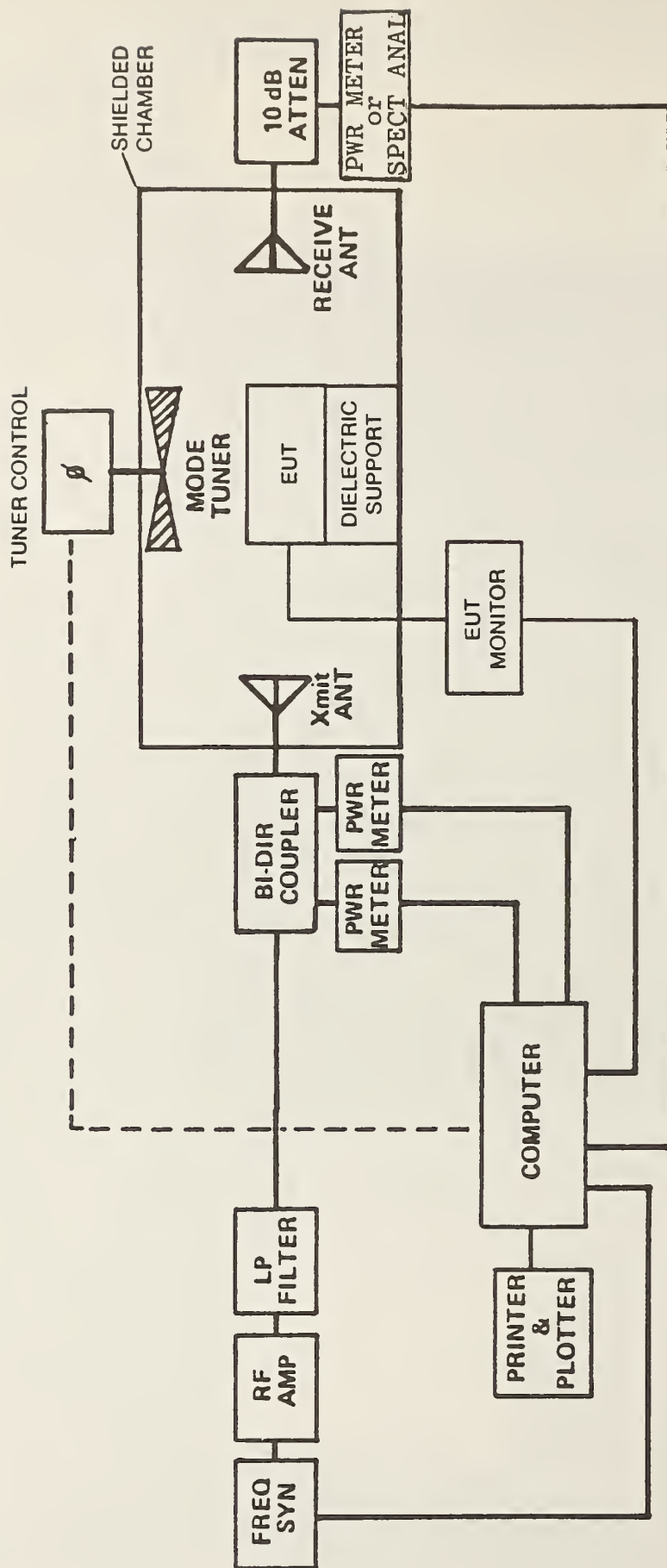
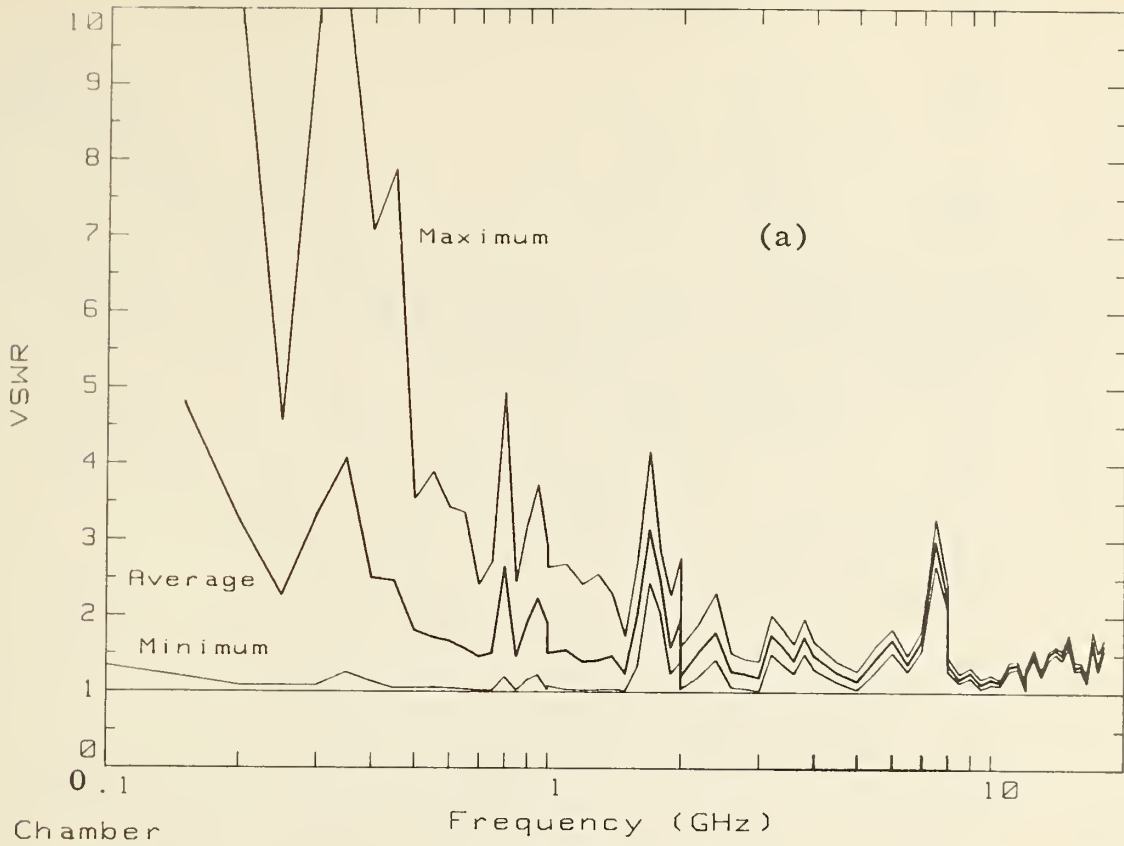


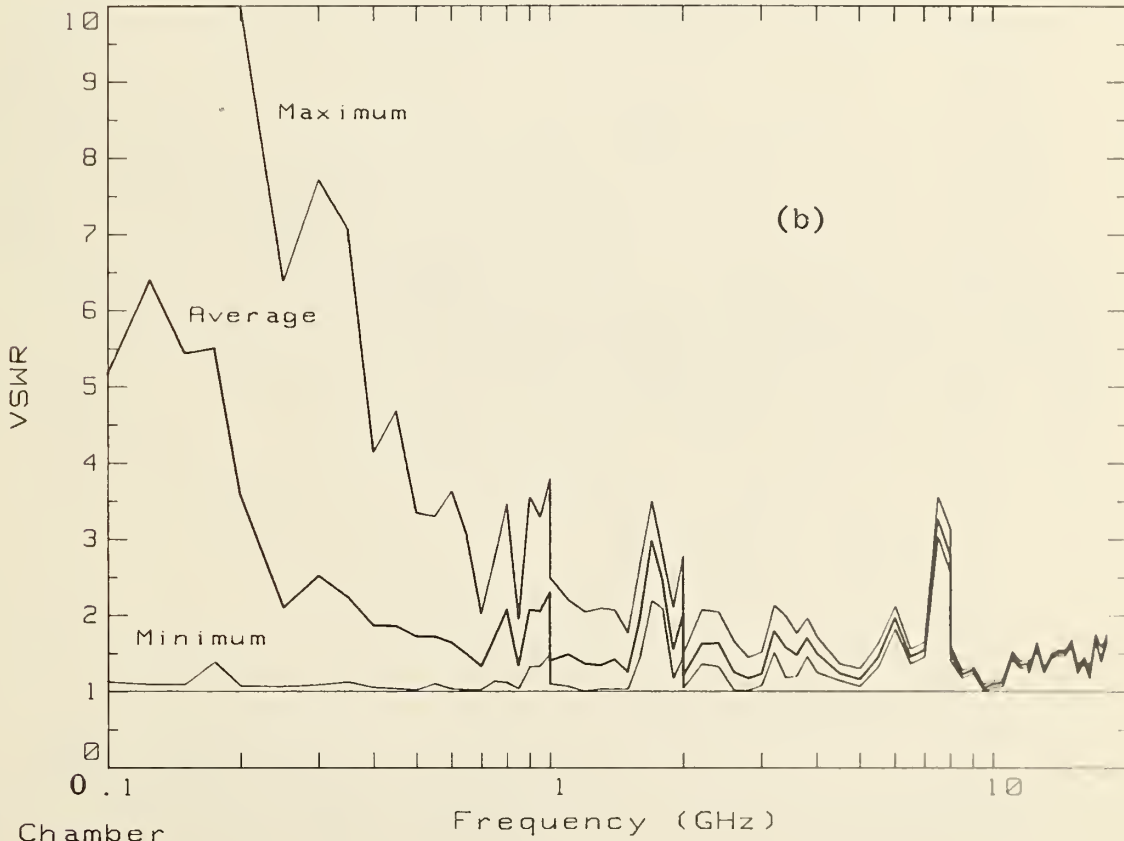
Figure 5. Block diagram of NBS system used in evaluation of NSWC reverberation chambers.

Composite VSWR of Transmit antennas in NSWC Chamber



Half Chamber

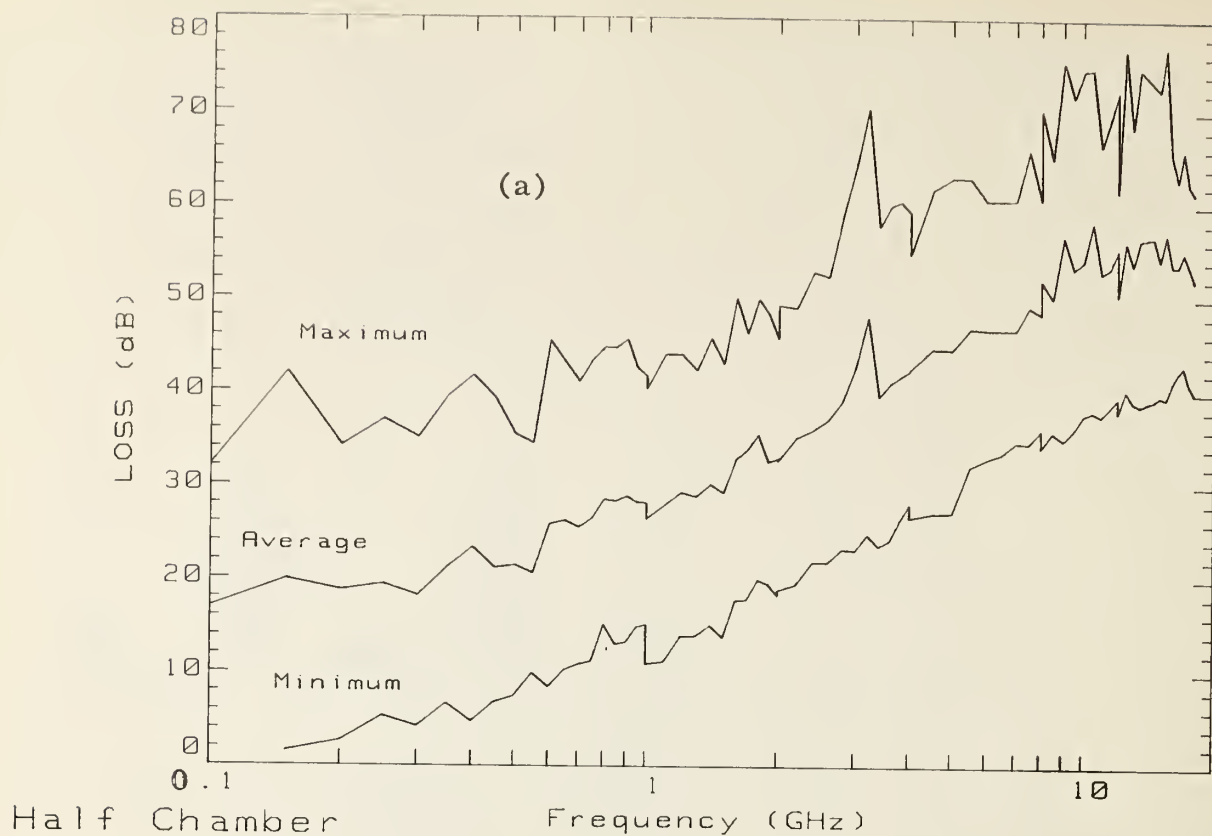
Composite VSWR of Transmit antennas in NSWC Chamber



Full Chamber

Figure 6. Statistical representation of the composite VSWR of the transmitting antennas used to launch the fields inside the NSWC reverberation chambers. (see table 1)

SYSTEM LOSS of NSWC Chamber



SYSTEM LOSS of NSWC Chamber

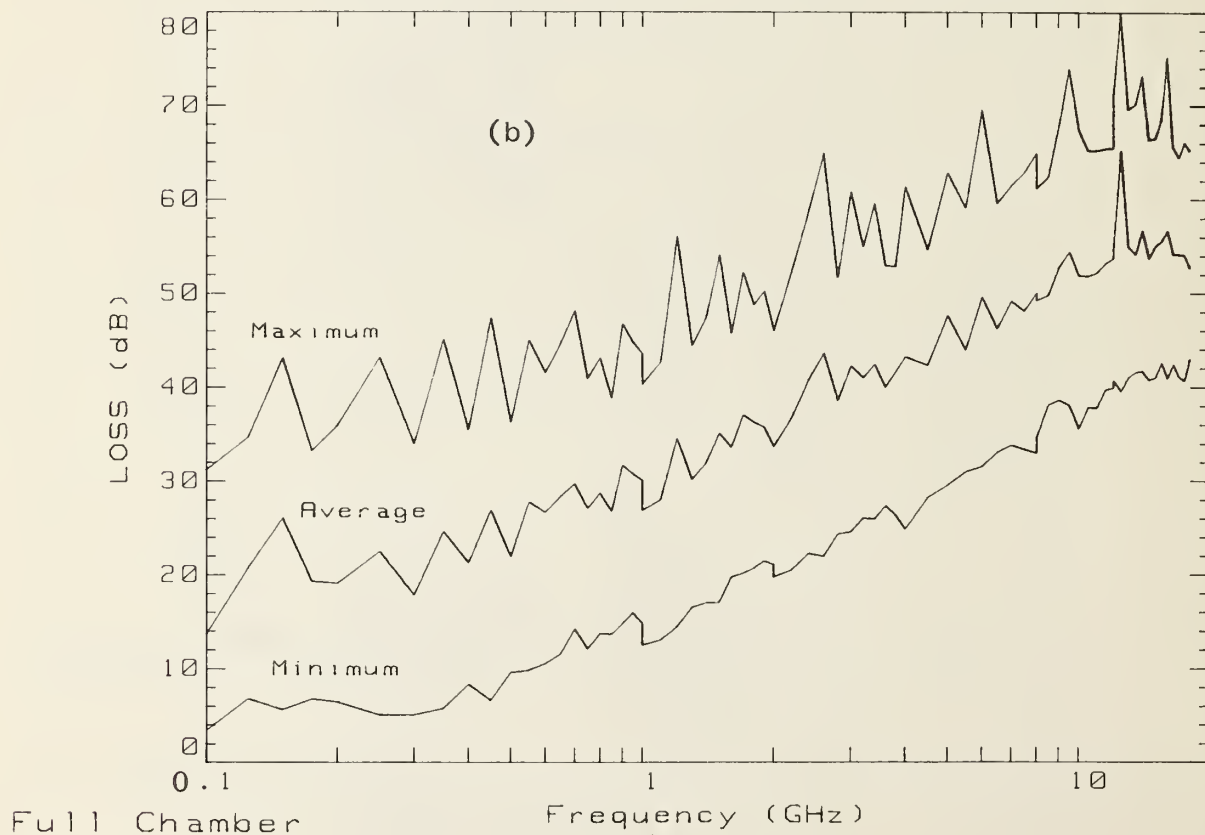
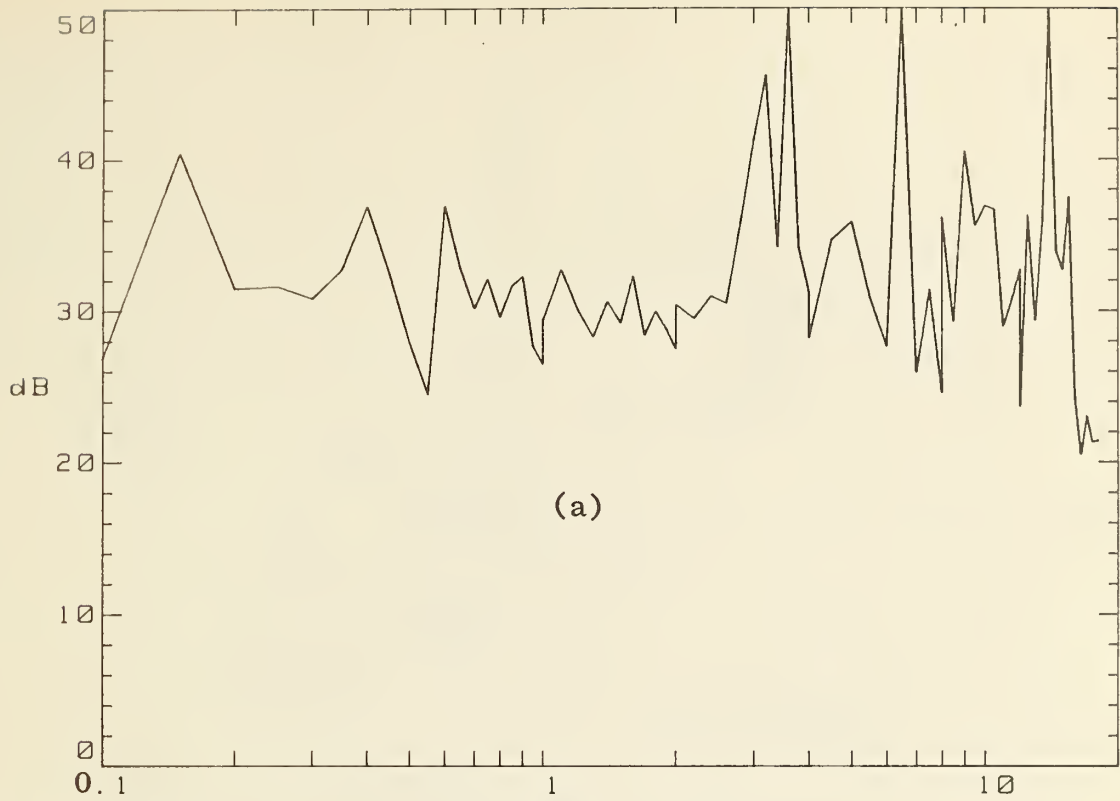


Figure 7. Coupling efficiency (maximum, average and minimum losses) between transmitted and received powers measured at antennas' terminals inside NSWC reverberation chambers. (see table 1 for definition of antennas used.)

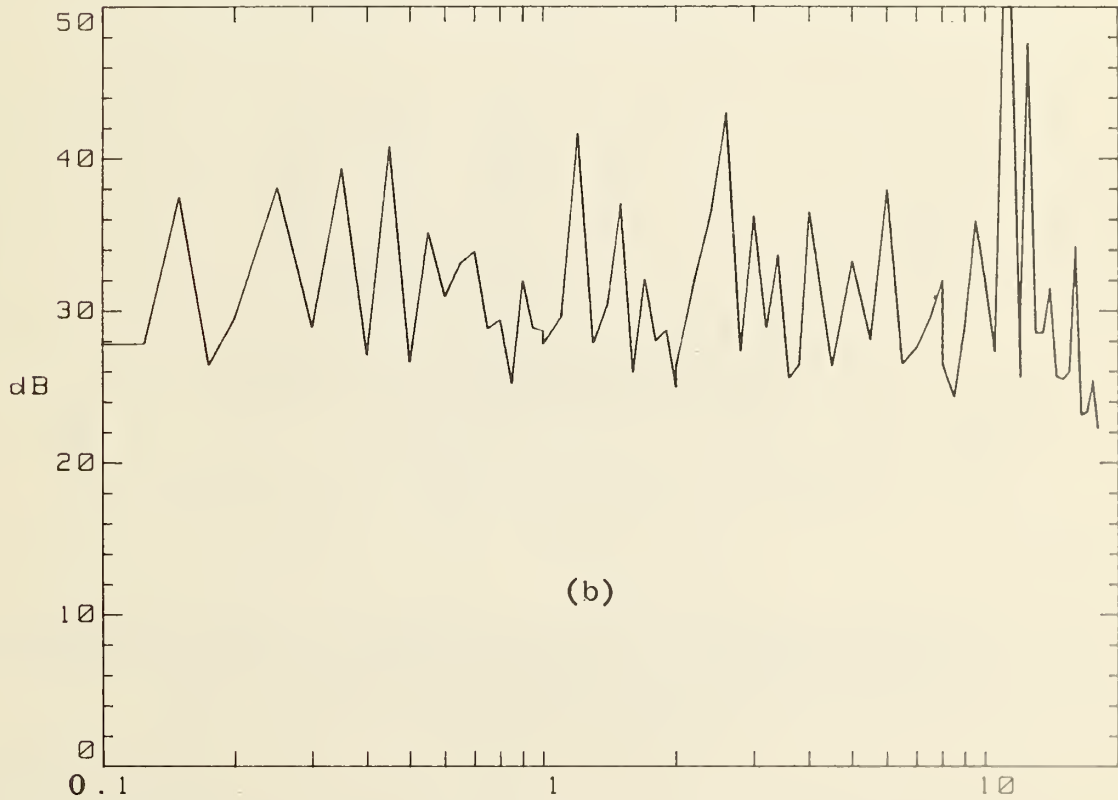
Tuner Effectiveness [$20 \times \text{Log}(E_{a \text{ max}}/E_{a \text{ min}})$]



NSWC Half Chamber

Frequency (GHz)

Tuner Effectiveness [$20 \times \text{Log}(E_{a \text{ max}}/E_{a \text{ min}})$]



NSWC Full Chamber

Frequency (GHz)

Figure 8. Ratio of maximum to minimum received power obtained by rotating tuner(s) in the frequency range 100 MHz to 18 GHz inside the NSWC reverberation chambers.

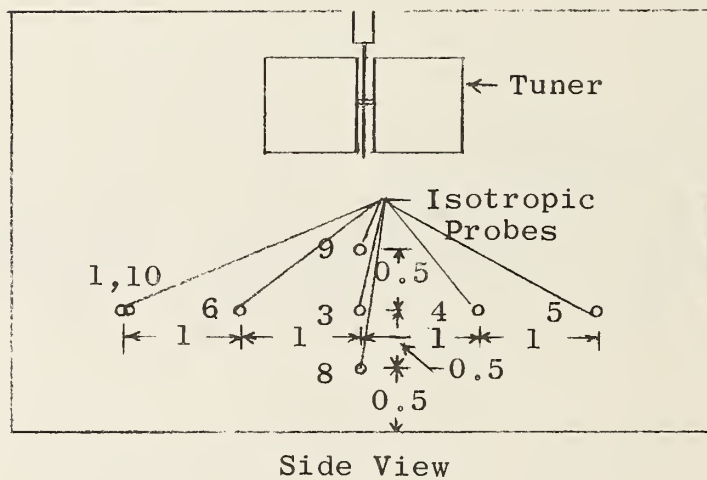
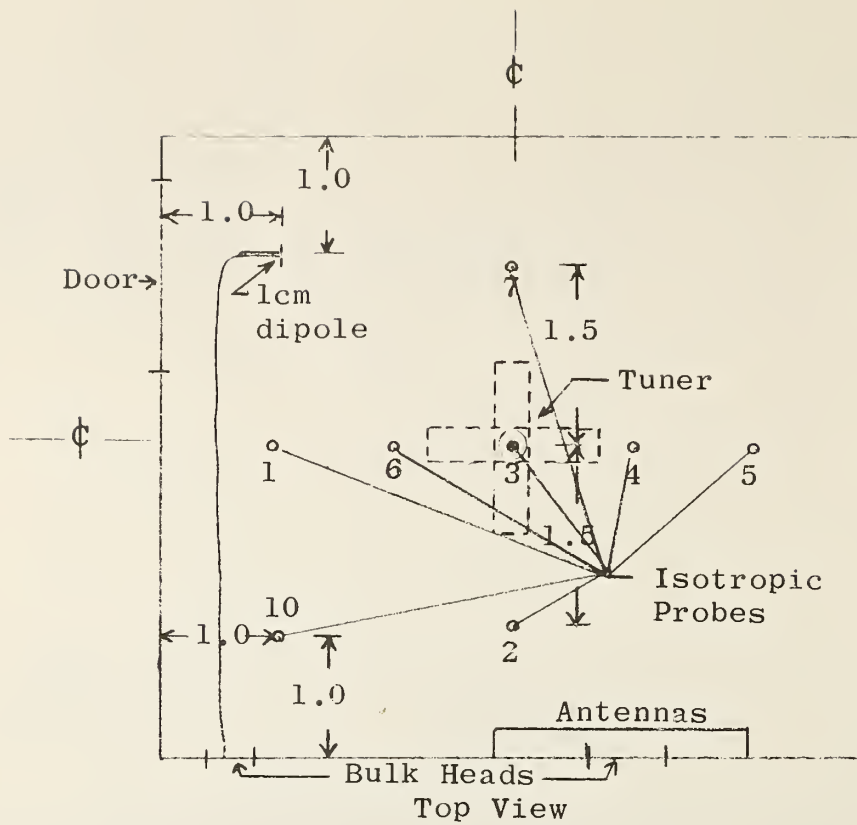


Figure 9a. Cross sectional views of NSWC half size reverberation chamber showing placement of NBS isotropic probes for evaluation of spatial distribution of E-fields.

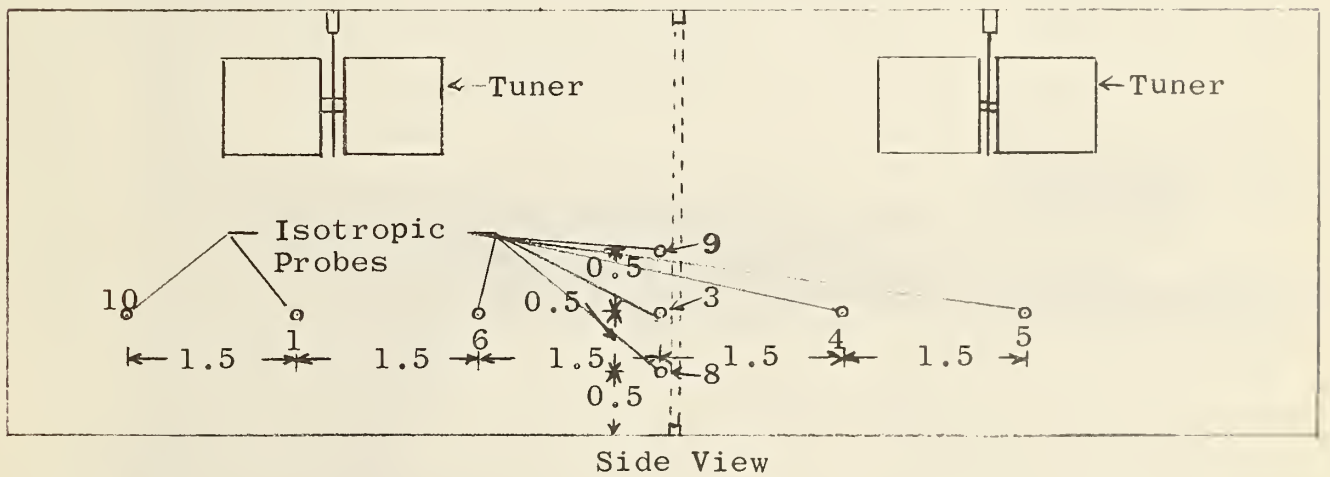
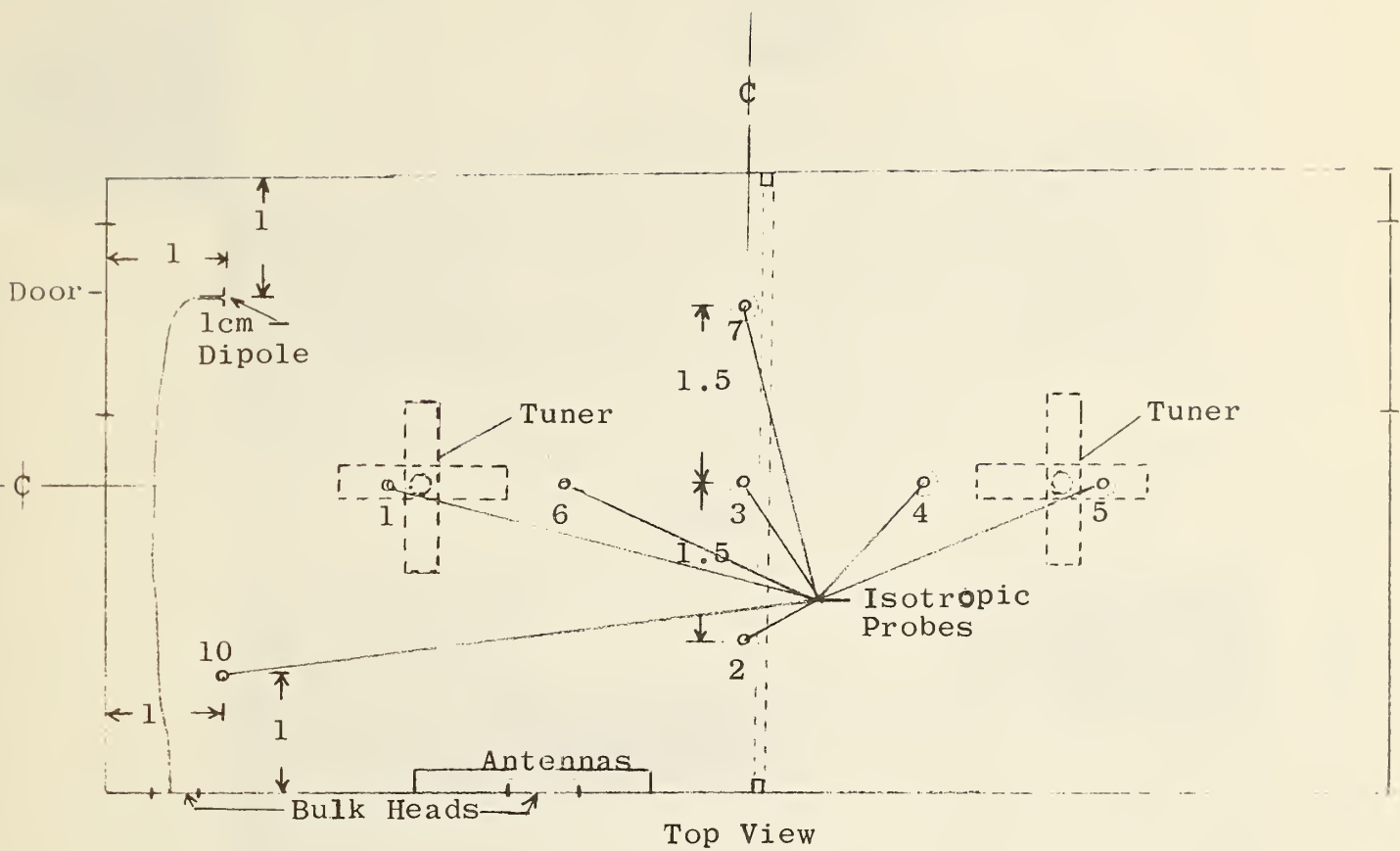


Figure 9b. Cross sectional views of NSWC full size reverberation chamber showing placement of NBS isotropic probes for evaluation of spatial distribution of E-fields.

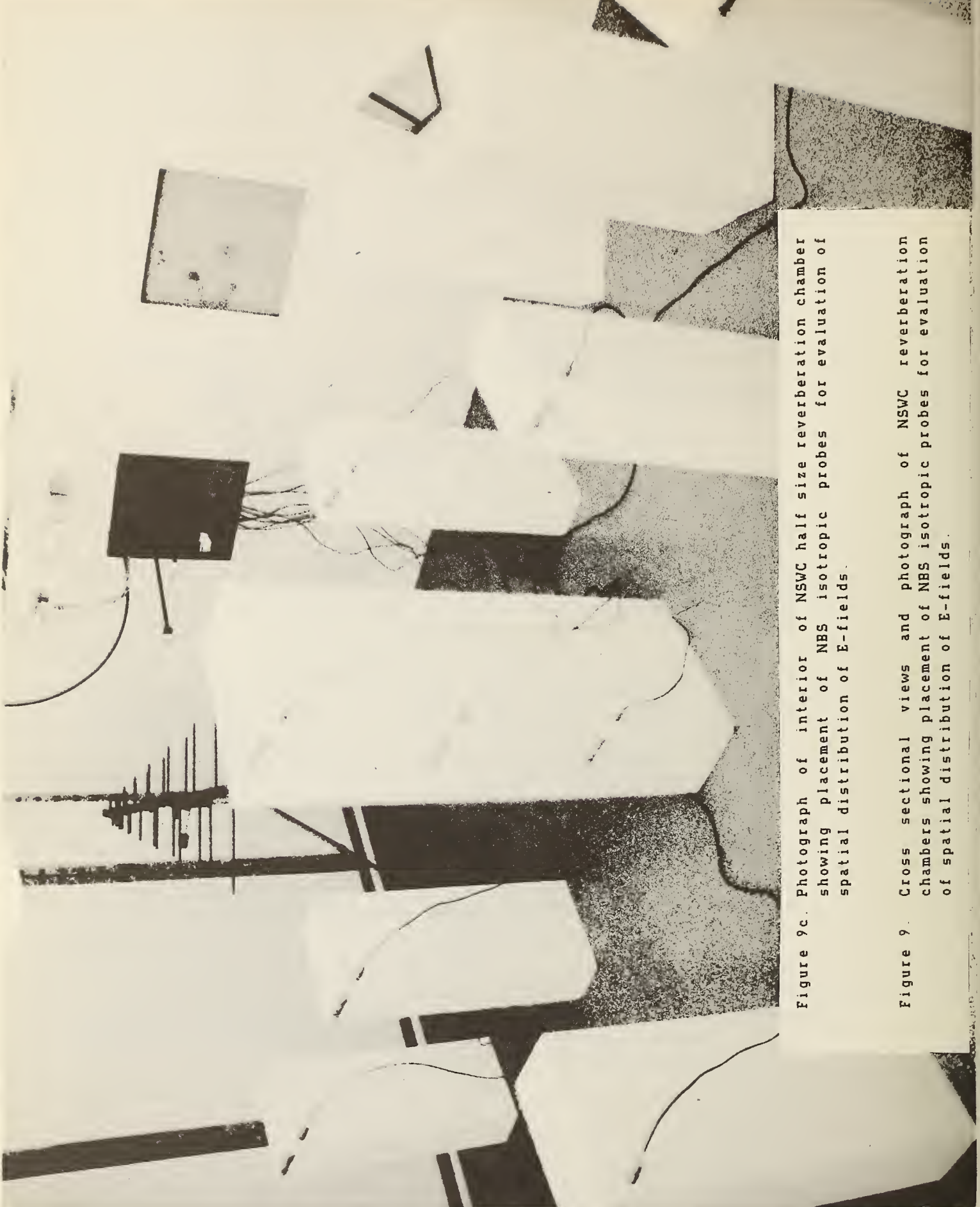


Figure 9c. Photograph of interior of NSWC half size reverberation chamber showing placement of NBS isotropic probes for evaluation of spatial distribution of E-fields.

Figure 9. Cross sectional views and photograph of NSWC reverberation chambers showing placement of NBS isotropic probes for evaluation of spatial distribution of E-fields.

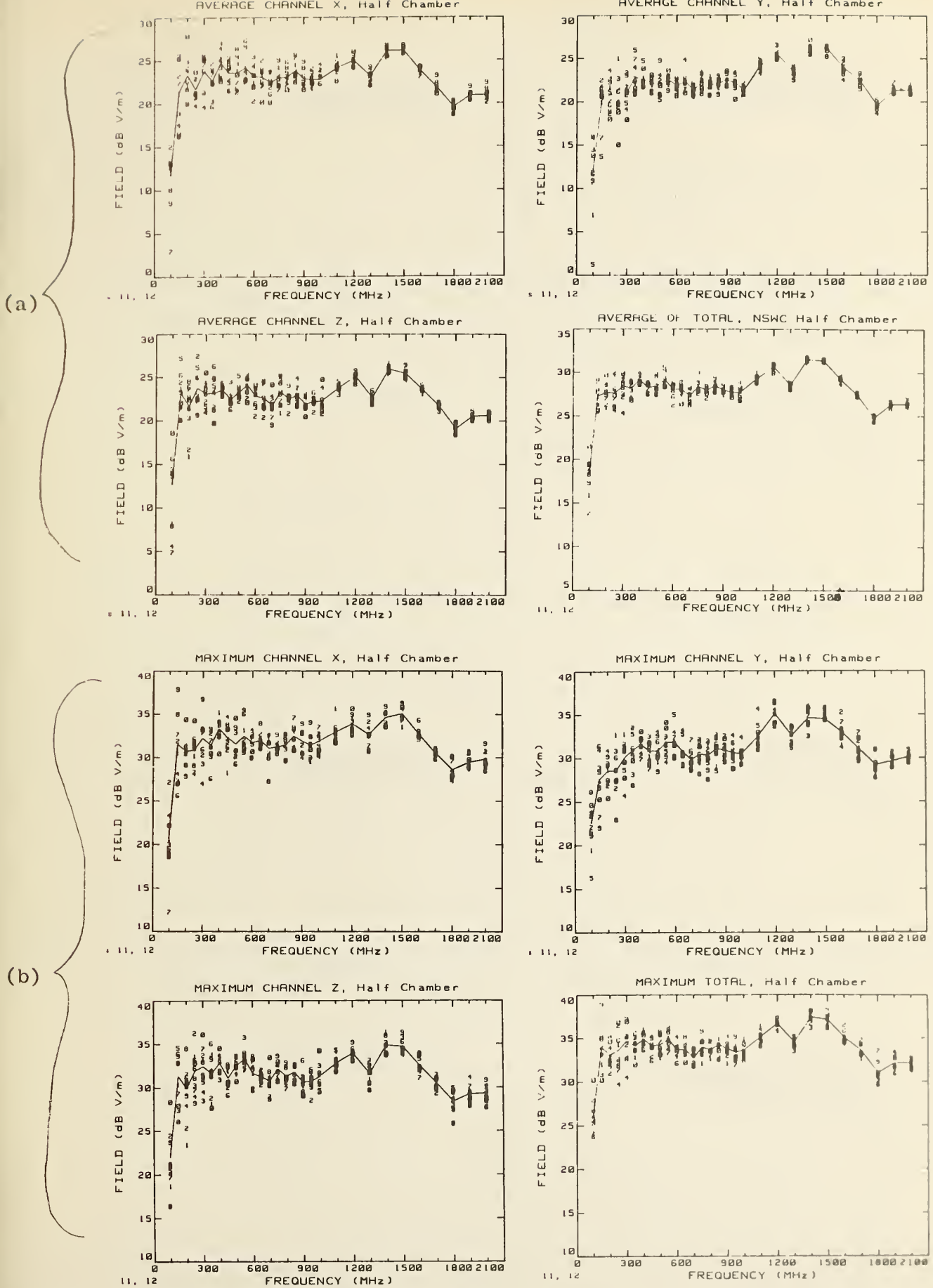


Figure 10. Spatial distribution of the E-field measured inside the NSWC half reverberation chamber using array of 10 NBS isotropic probes: (a) average, and (b) maximum. Net input power normalized to 1 watt. Transmitting antennas are log periodic, 0.1 GHz to 1.0 GHz, and low power horn, 1.0 GHz to 2.0 GHz.

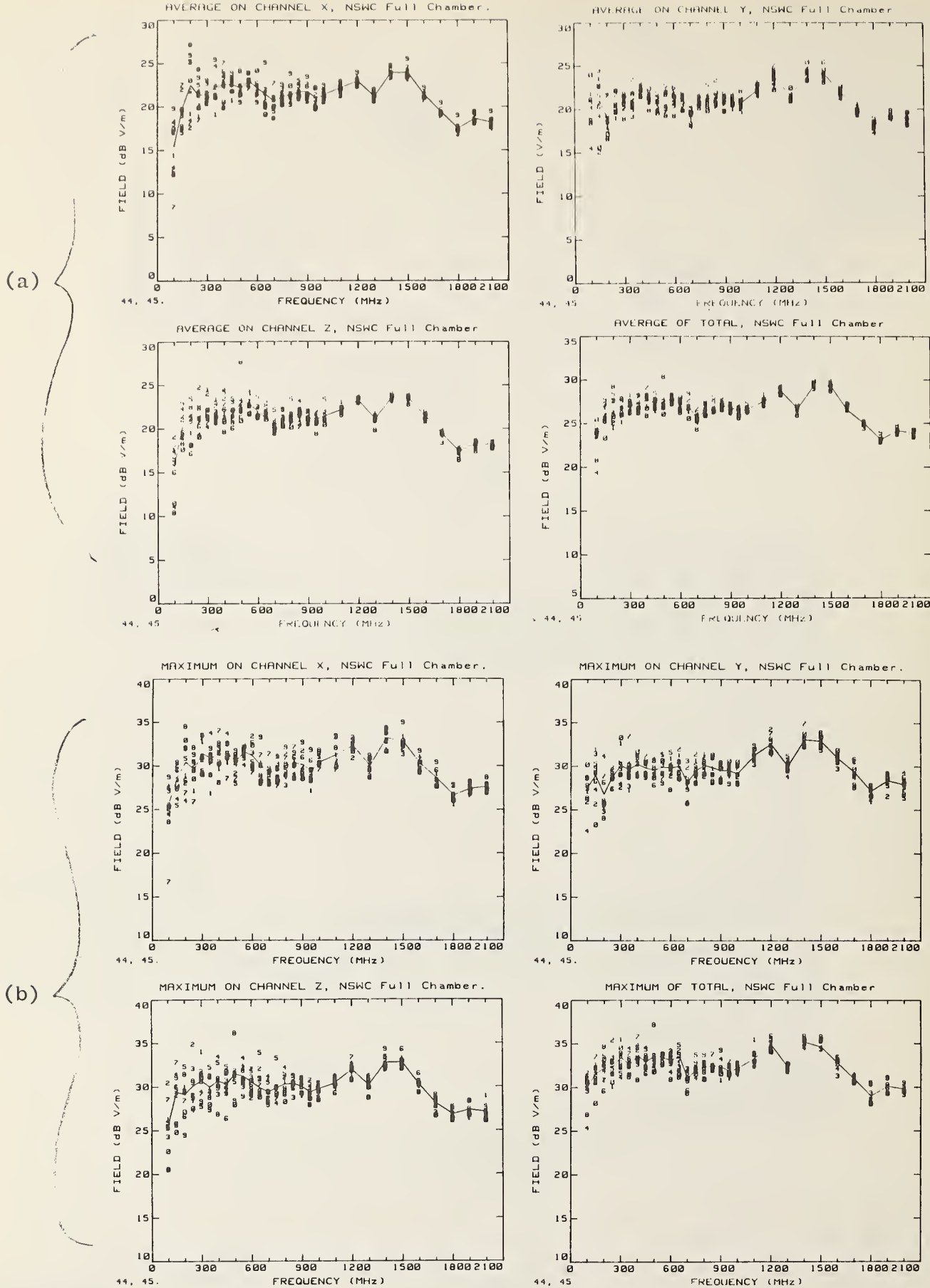


Figure 11. Spatial distribution of the E-field measured inside NSWC full reverberation chamber using array of 10 NBS isotropic probes: (a) average, and (b) maximum. Net input power normalized to 1 watt. Transmitting antennas same as figure 10.

(a)

(b)

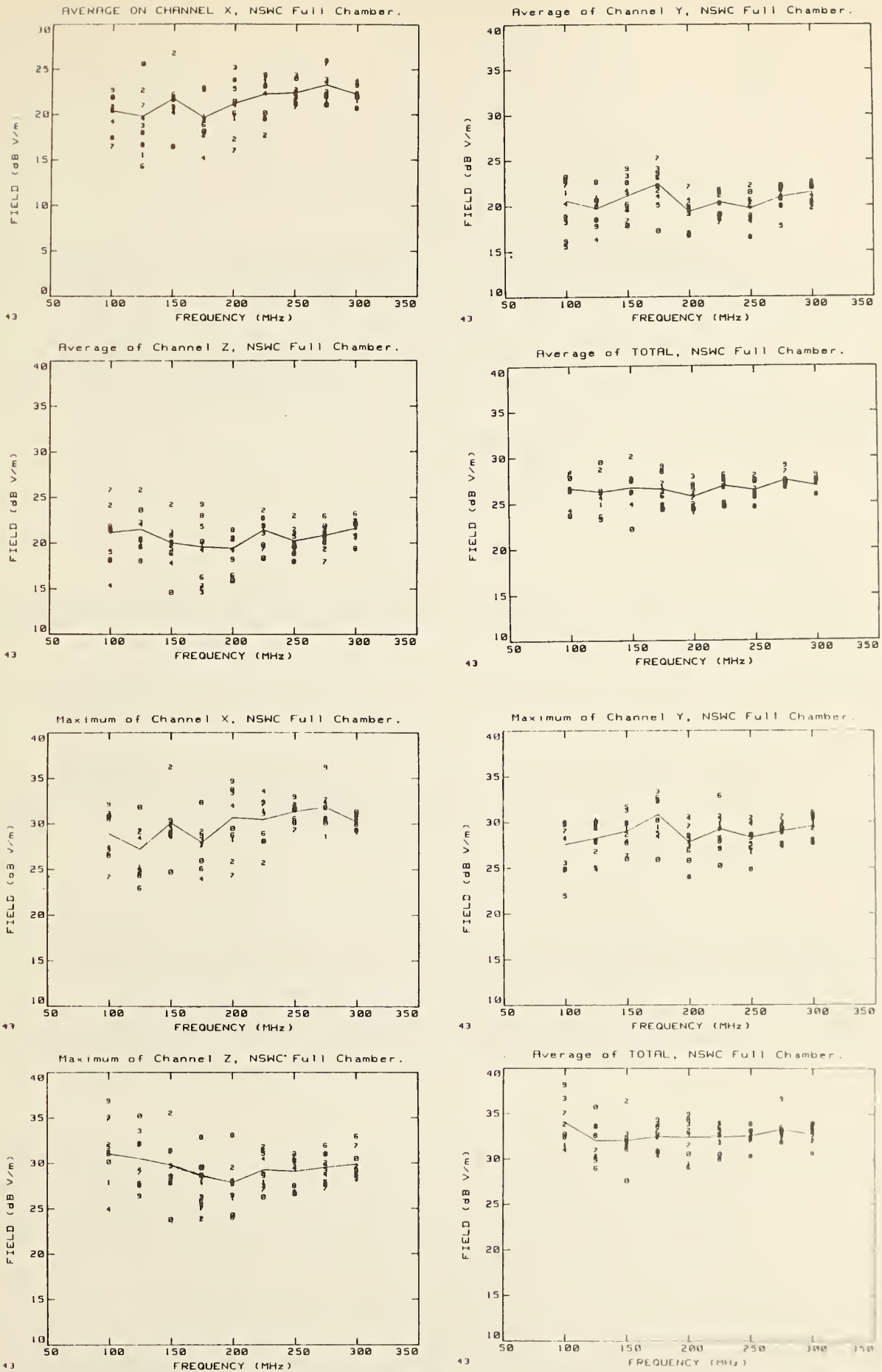


Figure 12. Spatial distribution of the E-field measured inside NSWC full reverberation chamber using array of 10 NBS isotropic probes, 100 MHz to 300 MHz: (a) average, and (b) maximum. Net input power normalized to 1 watt. Log periodic transmitting antenna replaced by Cavitenna.

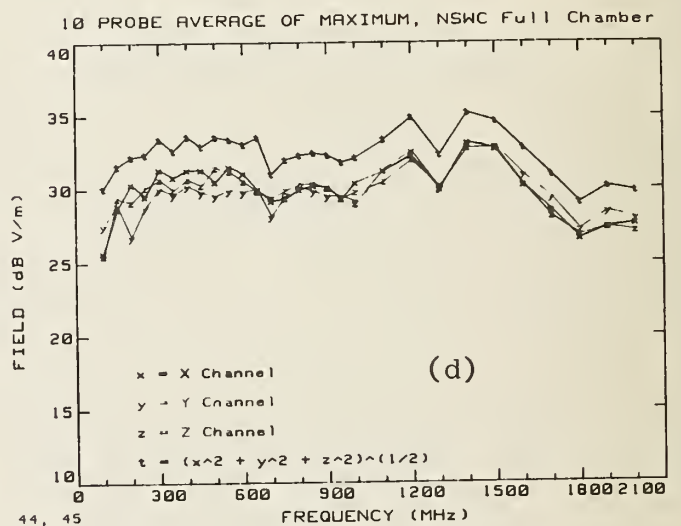
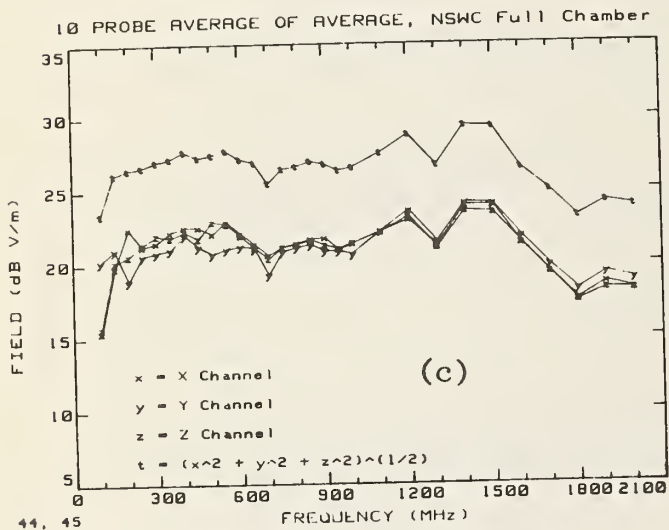
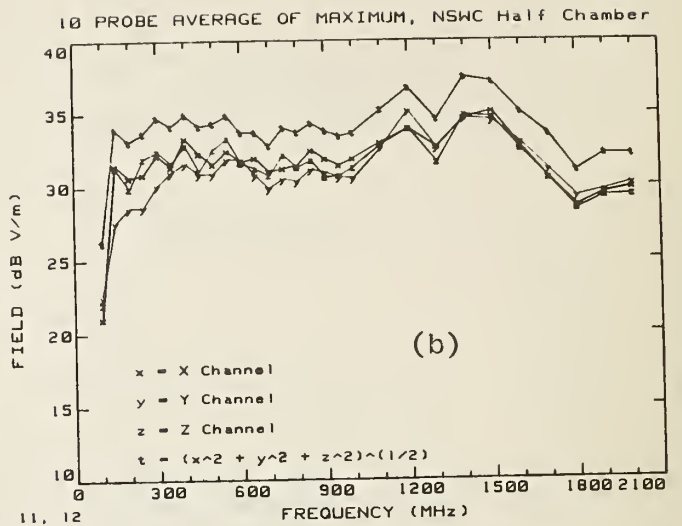
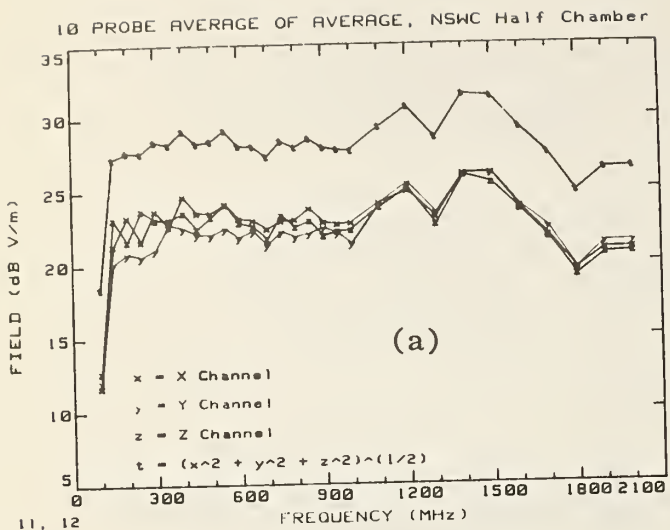


Figure 13. Average values of the E-field strength measured inside NSWC reverberation chambers using array of 10 NBS isotropic probes with 1 watt net input power: (a) and (c) average of the averages, (b) and (d) average of the maximums. Transmitting antennas same as figure 10.

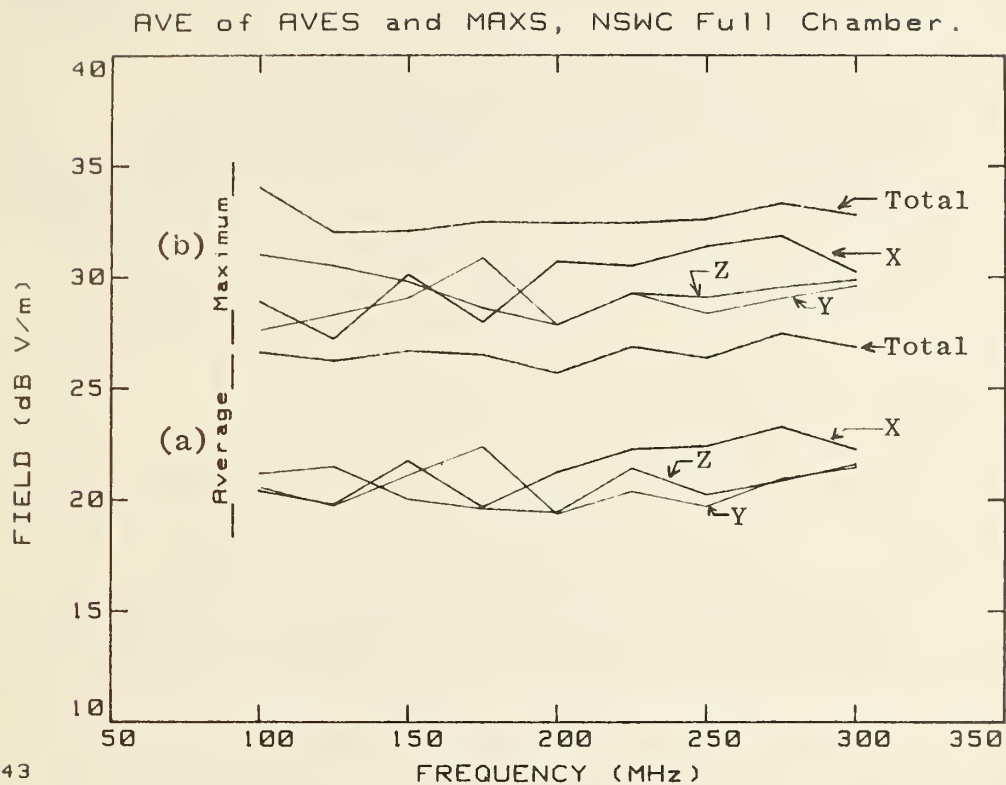
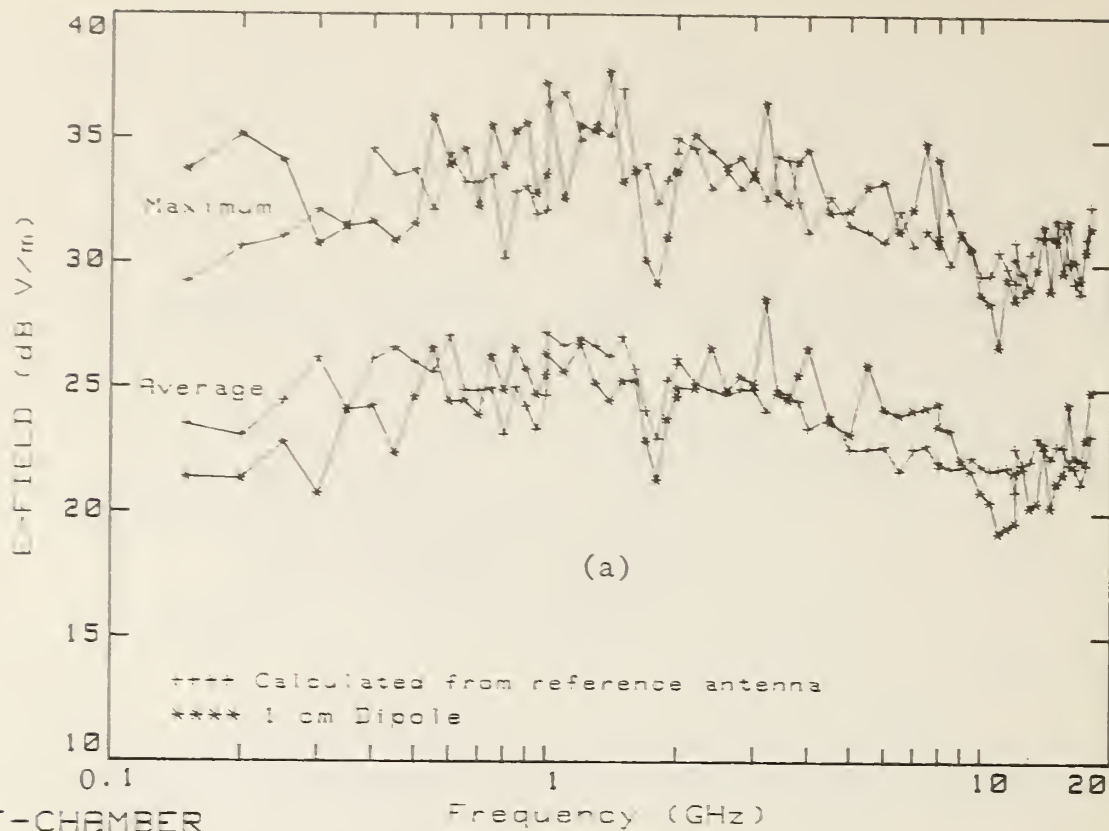


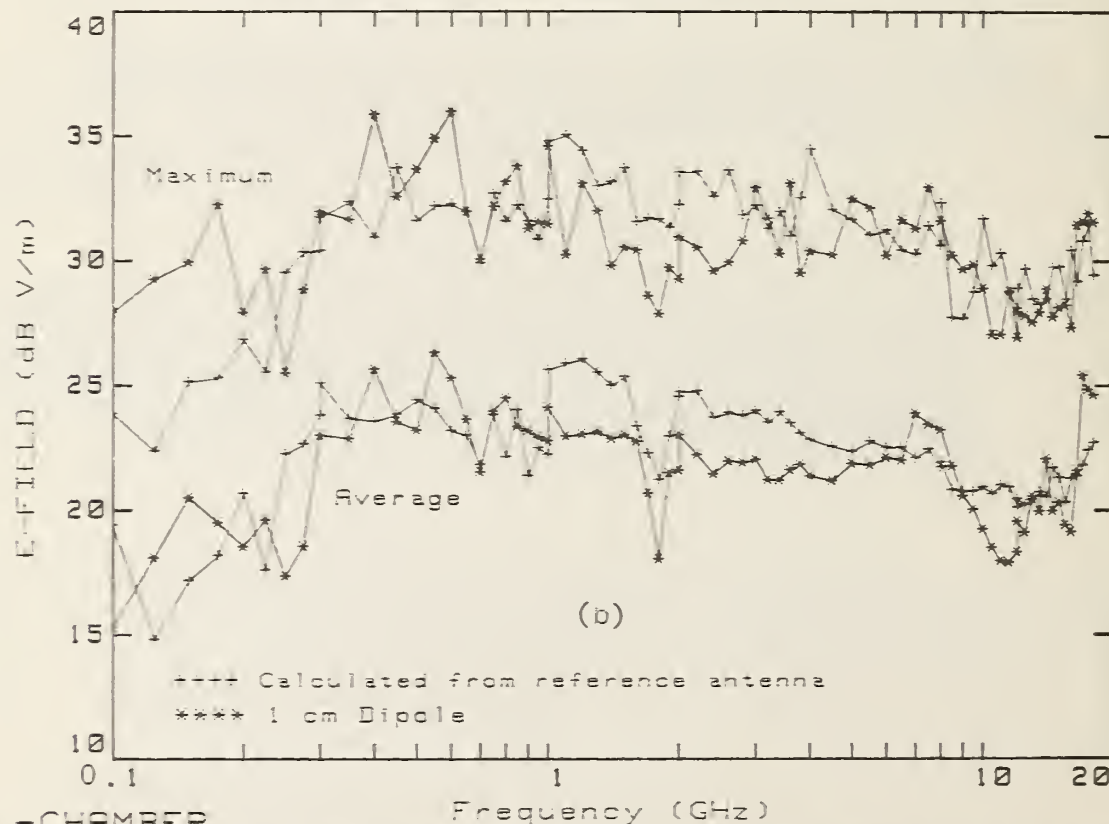
Figure 14. Average values of the E-field strength measured inside NSWC full reverberation chamber using array of 10 NBS isotropic probes, 100 MHz to 300 MHz: (a) average of the averages, (b) average of the maximums. Net input power normalized to 1 watt. Log periodic transmitting antenna replaced with cavitenna.

CALCULATED FIELD AND 1cm DIPOLE



HALF-CHAMBER

CALCULATED FIELD AND 1cm DIPOLE



FULL-CHAMBER

Figure 15. Average and maximum E-field strength determined inside NSWC reverberation chambers using: (1) composite of three receiving antennas (see table 1) received power measurements, and (2) calibrated 1 cm dipole probe measurements. Net input power normalized to 1 watt.

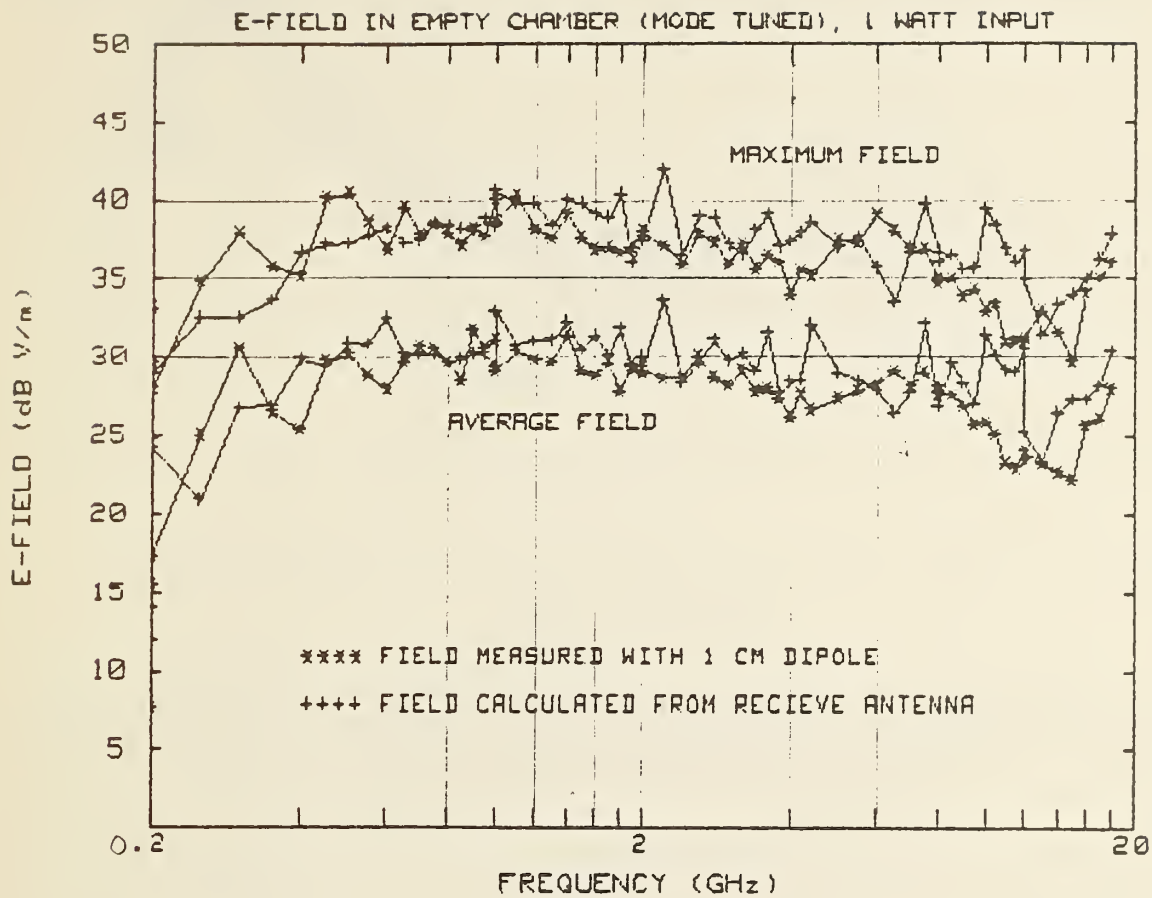
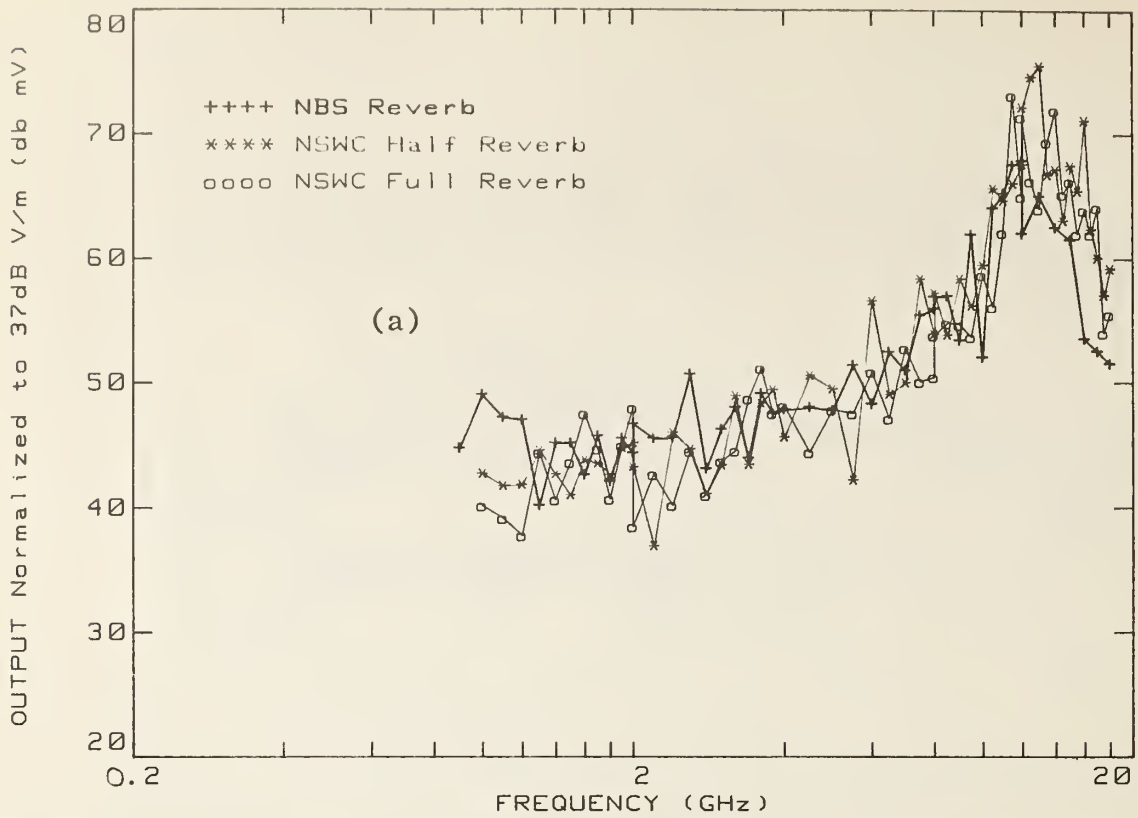


Figure 16. Average and maximum E-field strength inside empty NBS reverberation chamber for 1 watt net input power determined from: (1) composite of 3 antennas received power measurements, and (2) calibrated 1 cm dipole probe measurements.

PEAK RESPONSE of 1cm DIPOLE in VARIOUS CHAMBERS



PEAK RESPONSE of RIDGED HORN in VARIOUS CHAMBERS

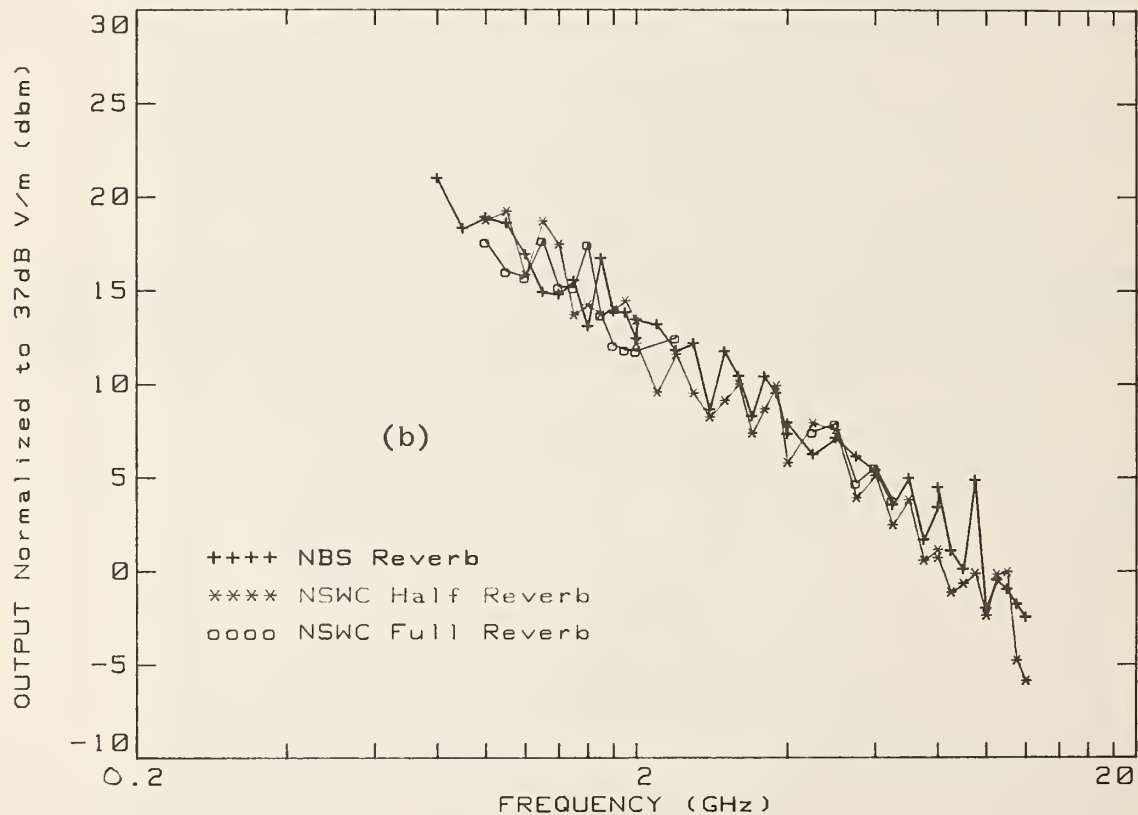


Figure 17. Comparison of the peak responses of NBS 1 cm dipole probe and NBS single ridged horn to normalized E-field of 37 dB V/m determined using NBS and NSWC reverberation chambers. (a) 1 cm dipole probe, (b) ridged horn.

Table 1. Transmitting and receiving antennas used in NSWC reverberation chambers evaluation

Frequency (GHz)	Transmitting	Receiving
0.1 - 0.2	Cavitenna	Log Periodic *
0.2 - 1.0	Log Periodic	Log Spiral
1.0 - 2.0	1-2 GHz Lo.Pwr. Horn	NBS Rect. Ridged Horn
2.0 - 4.0	2-4 GHz Lo.Pwr. Horn	NBS Rect. Ridged Horn
4.0 - 8.0	4-8 GHz Lo.Pwr. Horn	NBS Double Ridged Cir. Horn
8.0 - 12.0	8-12 GHz Lo.Pwr. Horn	NBS Double Ridged Cir. Horn
12.0 - 18.0	12-18 GHz Lo.Pwr. Horn	NBS Double Ridged Cir. Horn

* Used out of band. Recommend use of appropriate (in band) antenna.

Table 2. Spatial variations in the E-field average and maximum values measured inside the NSWC reverberation chambers

Frequency (GHz)	Variation in E-field (dB)	
	Half Chamber	Full Chamber
100	< ± 8.0	< ± 7.0
150	< ± 7.0	< ± 6.0
200	< ± 5.5	< ± 5.0
300	< ± 4.0	< ± 3.5
500	< ± 3.0	< ± 3.0
1000	< ± 2.5	< ± 2.3
2000	< ± 2.0	< ± 1.8

Table 3. Summary and estimates of measurement uncertainties for determining field strength inside NSWC reverberation chambers - Mode Tuned (100 MHz - 2.0 GHz)

Source of Error	Error (dB)											
	100 MHz		150 MHz		200 MHz		500 MHz		1.0 GHz		2.0 GHz	
	Ave.	Max.	Ave.	Max.	Ave.	Max.	Ave.	Max.	Ave.	Max.	Ave.	Max.
<u>1a. Received Power</u>												
Cable Loss	± 0.05		± 0.05		± 0.05		± 0.05		± 0.05		± 0.10	
Attenuator Cal.	± 0.10		± 0.10		± 0.10		± 0.10		± 0.10		± 0.10	
Antenna Efficiency	± 0.05		± 0.05		± 0.05		± 0.05		± 0.05		± 0.10	
Pwr. Meter Cal.	± 0.20		± 0.20		± 0.20		± 0.20		± 0.20		± 0.20	
Sub Total	± 0.40		± 0.40		± 0.40		± 0.40		± 0.40		± 0.50	
Mismatch	-5.2	-10.6	-4.4	-8.7	-3.4	-6.7	-1.5	-3.4	-1.1	-2.2	-1.3	-1.7
<u>1b. E-Field Meas.</u>												
1cm dipole probe	----- ± 1.0 -----											
<u>2. Sampling</u>												
Efficiency												
Spatial Field Var.	± 8.0		± 7.0		± 6.0		± 3.0		± 2.5		± 1.5	
Limited Sample Size (see [1])	±0.2	±0.5	±0.2	±0.5	±0.2	±0.5	±0.2	±0.5	±0.2	±1.5	±0.3	±1.0
Sub Total	±8.2	±8.5	±7.2	±7.5	±6.2	±6.5	±3.2	±3.5	±2.7	±4.0	±1.8	±2.5
<u>3. Wave Impedance</u>												
(see [1])	-2.8	-2.8	-2.4	-2.4	-2.0	-2.0	-2.0	-2.0	-2.0	-2.0	-2.0	-2.0
	+2.0	+6.0	+2.0	+6.0	+2.0	+6.0	+2.0	+4.5	+2.0	+3.0	+2.0	+3.0
<u>E-Field Determined</u>												
<u>By Receiving Ant.</u>												
Total Worst	-16.6	-22.3	-14.4	-19	-12	-15.6	-7.1	-9.3	-6.2	-8.6	-5.6	-6.7
Case Error	+10.6	+14.9	+9.2	+13.9	+8.6	+12.9	+5.6	+8.4	+5.1	+7.4	+4.3	+6.0
RSS Error	-10.1	-13.8	-8.8	-11.7	-7.4	-9.6	-4.1	-5.3	-3.6	-5.0	-3.0	-3.7
	+8.5	+10.4	+7.5	+9.6	+6.5	+8.9	+3.8	+5.3	+3.4	+5.0	+2.7	+3.9
<u>E-Field Determined</u>												
<u>By Dipole Probe</u>												
Total Worst	-12.0	-12.3	-10.6	-11	-9.2	-9.5	-6.2	-6.5	-5.7	-7.0	-4.8	-5.5
Case Error	+11.2	+15.5	+10.2	+14	+9.2	+13.5	+6.2	+9.0	+5.7	+8.0	+4.8	+6.5
RSS Error	-8.7	-9.0	-7.7	-7.9	-6.6	-6.9	-3.9	-4.2	-3.5	-4.6	-2.9	-3.4
	+8.5	+10.5	+7.5	+9.7	+6.6	+8.7	+3.9	+5.8	+3.5	+5.1	+2.9	+4.0

Table 4. Summary and estimates of measurement uncertainties for determining field strength inside NSWC reverberation chambers - Mode Stirred (1.0 GHz - 18.0 GHz)

Source of Error	Error (dB)											
	1.0 GHz		2.0 GHz		4.0 GHz		8.0 GHz		12.0 GHz		18.0 GHz	
	Ave.	Max.	Ave.	Max.	Ave.	Max.	Ave.	Max.	Ave.	Max.	Ave.	Max.
1a. Received Power												
Cable Loss	± 0.05		± 0.10		± 0.10		± 0.15		± 0.15		± 0.20	
Atten. Calibration	± 0.10		± 0.10		± 0.15		± 0.15		± 0.20		± 0.20	
Antenna Efficiency	± 0.05		± 0.10		± 0.15		± 0.15		± 0.20		± 0.20	
Spec. Analyzer Cal.	± 1.00		± 1.00		± 1.50		± 1.50		± 1.50		± 1.50	
Sub Total	± 1.20		± 1.30		± 1.90		± 1.95		± 2.05		± 2.10	
Mismatch	-1.3	-2.4	-1.2	-1.7	-0.8	-1.3	-1.5	-1.7	-0.5		-1.0	
1b. E-Field Meas.												
1cm Dipole Probe	± 1.0		± 1.0		± 1.5		± 1.5		± 2.0		± 2.0	
2. Sampling Efficiency												
Spatial Field Var.	± 2.5		± 1.5		± 1.0		± 0.5		± 0.5		± 0.5	
Limited Sample Size (see [1])	±0.1	±0.2	±0.1	±0.3	±0.2	±0.5	±0.3	±0.7	±0.3	±1.0	±0.3	±1.5
Sub Total	±2.6	±2.7	±1.6	±1.8	±1.2	±1.5	±0.8	±1.5	±0.8	±1.5	±0.8	±2.2
3. Wave Imped ≠ 120π	Average ≤ ±2.0, -2.0 ≤ Maximum ≤ +3.0											
4. Input Power Var.	-1.3	-2.4	-1.2	-1.7	-0.8	-1.3	-1.6		-0.5		-1.0	
E-Field Determined By Receiving Ant.												
Total Worst Case Error	-8.4	-10.7	-7.3	-8.5	-6.7	-8.0	-7.9	-8.8	-5.9	-6.6	-6.9	-8.3
	+5.8	+6.9	+4.9	+6.1	+5.1	+6.4	+4.8	+6.5	+4.9	+6.6	+6.9	+7.3
RSS Error	-4.0	-4.9	-3.3	-3.8	-3.2	-3.6	-3.6	-3.9	-3.1	-3.3	-3.3	-3.9
	+3.5	+4.2	+2.9	+3.7	+2.9	+3.9	+2.9	+3.9	+3.0	+3.9	+3.0	+4.3
E-Field Determined By Dipole Probe												
Total Worst Case Error	-6.9	-8.9	-5.8	-6.5	-5.5	-6.3	-5.9	-6.6	-5.3	-6.0	-5.8	-7.2
	+5.6	+6.7	+4.6	+5.8	+4.7	+6.0	+4.3	+6.0	+4.8	+6.5	+4.8	+7.2
RSS Error	-3.7	-4.3	-3.0	-3.3	-2.9	-3.2	-3.1	-3.3	-3.0	-3.2	-3.1	-3.7
	+3.4	+4.2	+2.8	+3.6	+2.8	+3.7	+2.6	+3.7	+2.9	+3.9	+2.9	+4.2

Table 5. Estimates of impedance mismatch uncertainties for received power measurements for NSWC reverberation chambers

Frequency GHz	VSWR		Load Max	Mismatch Error (dB)	
	Source Ave	Max		Ave	Max
0.1	10.0	40.0	1.10	-5.15	-10.6
0.15	8.0	25.0	1.10	-4.36	-8.68
0.2	6.0	15.0	1.10	-3.40	-6.67
0.3	4.0	10.0	1.10	-2.19	-5.15
0.5	3.0	6.0	1.10	-1.46	-3.40
1.0	2.5	4.0	1.10	-1.07	-2.19
1.0	2.5	4.0	1.20	-1.25	-2.44
2.0	2.5	3.0	1.20	-1.25	-1.67
4.0	2.0	2.5	1.20	-0.81	-1.25
8.0	2.8	3.0	1.20	-1.51	-1.67
12.0	1.5	1.5	1.30	-0.48	-0.48
18.0	1.8	1.8	1.50	-1.03	-1.03

U.S. DEPT. OF COMM. BIBLIOGRAPHIC DATA SHEET <i>(See instructions)</i>	1. PUBLICATION OR REPORT NO. NBSIR 86-3051	2. Performing Organ. Report No.	3. Publication Date June 1986
4. TITLE AND SUBTITLE Electromagnetic Radiation Test Facilities Evaluation of Reverberation Chambers Located at NSWC, Dahlgren, Virginia			
5. AUTHOR(S) Myron L. Crawford and Galen H. Koepke			
6. PERFORMING ORGANIZATION <i>(If joint or other than NBS, see instructions)</i> NATIONAL BUREAU OF STANDARDS DEPARTMENT OF COMMERCE WASHINGTON, D.C. 20234		7. Contract/Grant No.	8. Type of Report & Period Covered
9. SPONSORING ORGANIZATION NAME AND COMPLETE ADDRESS <i>(Street, City, State, ZIP)</i>			
10. SUPPLEMENTARY NOTES <input type="checkbox"/> Document describes a computer program; SF-185, FIPS Software Summary, is attached.			
<p>This report describes measurement procedures and results obtained from evaluating the reverberation chamber facilities located at the Naval Surface Weapons Center (NSWC), Dahlgren, Virginia. The two chambers tested are referred to as 1) the half chamber, and 2) the full chamber. The facilities were developed by the NSWC for use in measuring and analyzing the electromagnetic susceptibility/vulnerability (EMS/V) of weapon systems and the shielding effectiveness of enclosures and shielding materials. A brief description of each facility is given including the instrumentation used for performing the evaluation and calibration of the facilities by the National Bureau of Standards (NBS). Measurements described include: 1) evaluation of the chambers' transmitting and receiving antennas' voltage standing wave ratios; 2) measurement of the chambers' insertion loss or coupling efficiency versus frequency; 3) measurement of the chambers' tuner effectiveness; 4) determination of the E-field uniformity in the chambers' test zones versus frequency; 5) determination of the absolute amplitude calibration of the test E-fields in the chambers based upon the reference antennas received power measurements and calibrated dipole probe antenna measurements; and 6) comparison of reference equipment under test (EUT) responses to test fields established inside the NSWC reverberation chambers and the NBS reverberation chamber. These results can then be compared to anechoic chamber results. Conclusions given indicate that the NSWC chambers can be used at frequencies down to approximately 150 MHz. Estimates are given of the measurement uncertainties derived empirically from the test results.</p>			
12. KEY WORDS <i>(Six to twelve entries; alphabetical order; capitalize only proper names; and separate key words by semicolons)</i> electromagnetic radiated susceptibility/vulnerability; reverberation chamber			
13. AVAILABILITY <input checked="" type="checkbox"/> Unlimited <input type="checkbox"/> For Official Distribution. Do Not Release to NTIS <input type="checkbox"/> Order From Superintendent of Documents, U.S. Government Printing Office, Washington, D.C. 20402. <input checked="" type="checkbox"/> Order From National Technical Information Service (NTIS), Springfield, VA. 22161		14. NO. OF PRINTED PAGES 44	15. Price

